Fluorescence of Organic Molecules in Chiral Recognition

Lin Pu

Department of Chemistry, University of Virginia, Charlottesville, Virginia 22904-4319

Received August 25, 2003

Contents

1. Introduction

Molecule-based fluorescent sensors are generally composed of a fluorophore and a binding site, and are incorporated with a signaling mode for the fluorophore in response to the event at the binding sites. A number of fluorescent signaling modes, such as quenching, enhancement, excimers, exciplexes, lifetimes, and anisotropy, are available for sensing. Fluorescence efficiency can be correlated with many structural features of chemicals including $\pi-\pi^*$ and $n-\pi^*$ transitions, structural rigidity, noncovalent interactions (e.g., hydrogen bonds, $\pi-\pi$ interactions, and hydrophilic and hydrophobic interactions), intra- or intermolecular energy transfers, and photoinduced electron transfers. These allow the development of fluorescent sensors with very diverse structures as well as specific responses for substrate detection. The high sensitivity of the fluorescence technique requires the use of only very small amounts of sensor molecules and/or analytes. By using optical fibers, fluorescence sensors can be further applied to continuous monitoring and remote sensing. A great number of fluorescent sensors have been constructed to detect protons, metal ions, anions, and neutral molecules.[1−3] Fluorescent sensors or labels have also been extensively applied in biological study.[4]

Chiral recognition in luminescence has been studied in the past two decades. By introducing chirality into the binding site, the resulting fluorescent sensor could carry out the enantioselective recognition of chiral organic molecules. Rapid determination of the enantiomeric composition of organic molecules is of great significance in drug discovery and catalyst screening, especially in connection with the application of the high throughput combinatorial technique. Several analytical tools such as electron spray mass spectroscopy, NMR, and electrophoresis are under investigation for this purpose.[5−9] Fluorescent sensors that are capable of differentiating the two enantiomers of a chiral compound should provide a real time technique in the rapid chiral assays with many unique advantages. Significant progress has been made in the development of enantioselective sensors. In this review article, we will make an effort to summarize the activity on the enantioselective fluorescent recognition studies. It is our wish that this

10.1021/cr030052h CCC: $48.50
Published on Web 02/03/2004

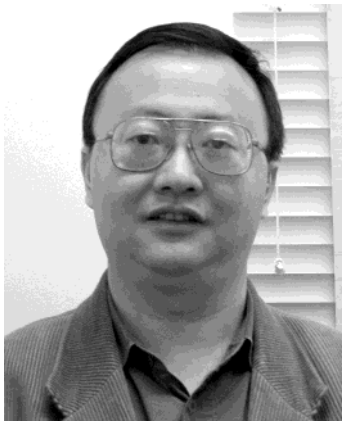

Lin Pu was born in 1965 in Xuyong, Sichuan Province, P. R. China. He received his B.S. degree in chemistry from Sichuan University in 1984. He then obtained the Doering Fellowship (the Chemistry Graduate Program of China) for graduate study in the U.S. and enrolled in the department of chemistry at University of California San Diego in 1985. Under the supervision of Professor Joseph M. O'Connor, he obtained his Ph.D. degree in 1990. From January 1991 to November 1992, he studied in Professor Henry Taube's laboratory at Stanford University as a postdoctoral fellow. From November 1992 to August 1994, he joined Professor Robert H. Grubbs's research group at California Institute of Technology to continue his postdoctoral training. In the fall of 1994, he was appointed as an assistant professor in the Department of Chemistry at North Dakota State University. In 1997, he moved to University of Virginia as an associate professor in the Department of Chemistry. He became a professor of chemistry at University of Virginia in 2003. The research projects in his laboratory focus on the design and synthesis of novel chiral molecules and macromolecules for applications in areas such as enantioselective fluorescent sensors, asymmetric catalysis, and electrical and optical materials.

paper could provide help to those who are interested in this growing and exciting research field. This review will only be limited to the discussion of organic fluorophores. References 10−20 provide some selected studies on the luminescence of inorganic compounds in chiral recognition.

2. Enantioselective Fluorescent Recognition of Chiral Amines and Amino Alcohols

Studying the chiral discrimination of organic fluorophores began with the work on their fluorescent responses to chiral amines and amino alcohols. These nitrogen-containing molecules often served as quenchers to reduce the fluorescent intensity of the fluorophores. Both dynamic and static fluorescence quenchings were observed. The dynamic quenching often involved the formation of an exciplex between the amines and the excited fluorophores, and the static quenching might be due to their nonfluorescent ground state hydrogen bonded complexes or the base-promoted deprotonation. In these studies, 1,1′-binaphthyl-based compounds were the most extensively used chiral receptors. The restricted rotation of the two naphthyl rings around their 1,1′-bond rendered these chiral atropisomers with high configurational stability. Their naphthyl rings also served as good fluorophores to signal the amine quenchers. Introduction of conjugated units to the binaphthyl rings led to amplification of their fluorescence signals. Besides the 1,1′-binaphthyl compounds, the responses of other fluorophores such as

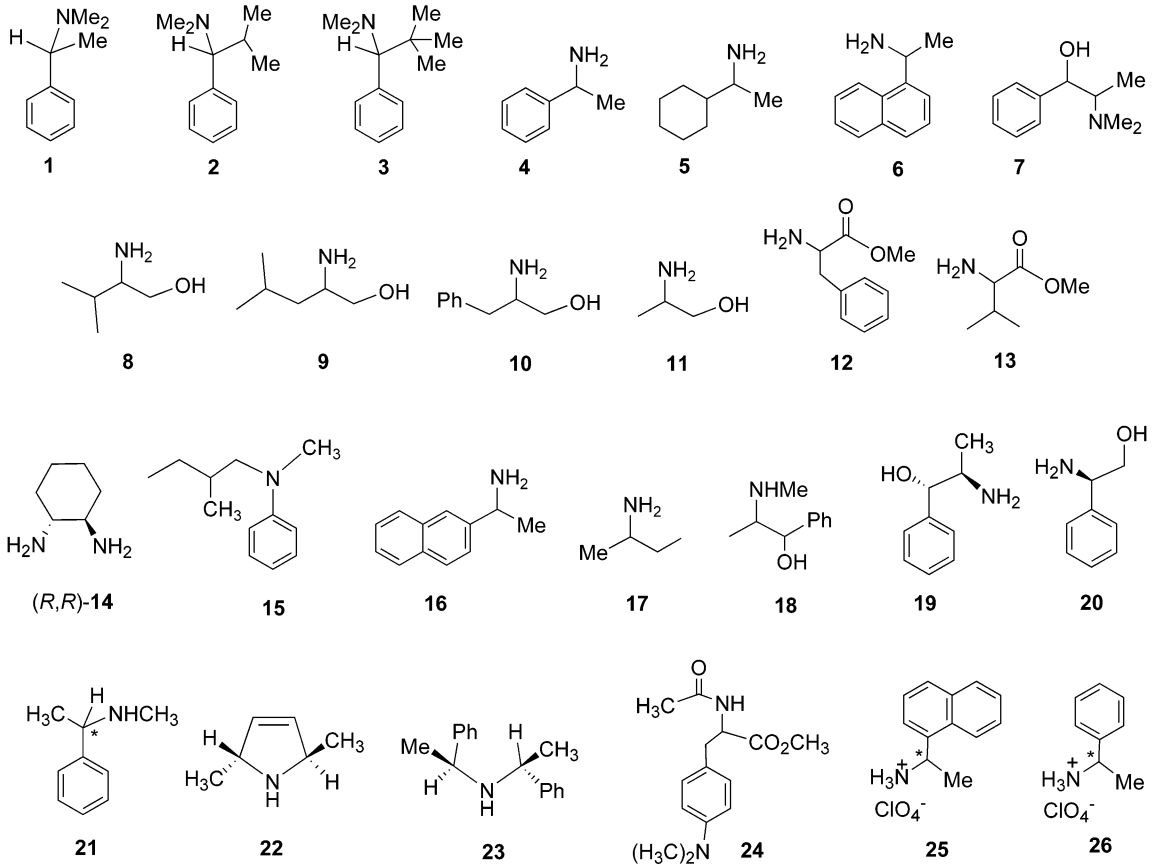

Figure 1. Chiral amines and amino alcohols studied.

helicenes, calixarenes, camphors, pyrenes, and crown ethers toward chiral amines and amino alcohols also exhibited various degrees of chiral discrimination. Figure 1 lists the structures of the chiral amines and amino alcohols discussed in this chapter.

2.1. 1,1′-Binaphthyl Fluorophores

2.1.1. Monomeric Binaphthyls

In 1978, Irie et al. reported the fluorescence quenching of 1,1′-binaphthyl (**27**) by the enantiomers of *N*,*N*-dimethyl-α-phenethylamine (**1**).[21] The fluorescence of racemic **27** at 360 nm ($\lambda_{exc} = 310$ nm) was

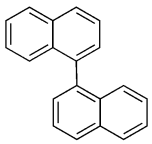

27

quenched at the same rate in *n*-hexane by both enantiomers of **1**. The fluorescence quenching followed the Stern−Volmer equation ($I_0/I = 1 + K_{SV}[Q] = 1 + k_q\tau_o[Q]$, where I and I_0 are the fluorescent intensity of the fluorophore with and without the quencher, [Q] is the concentration of the quencher, and K_{SV} is the Stern−Volmer constant; for dynamic quenching, K_{SV} is related to the fluorescence quenching rate constant k_q and the fluorescence lifetime τ_o; for static quenching, K_{SV} represents the association constant of the fluorophore with the quencher).[22] It was similar to a typical exciplex-type dynamic quenching, and the emission of the exciplex emission was extremely weak.

When (*R*)-(−)-**27** (1.1×10^{-5} M) with an optical purity of 77.5% was used, there was a significant difference in its fluorescence quenching by the (*R*)- and (*S*)-enantiomers of **1** (1×10^{-2} to 4.5×10^{-2} M). It was found that the ratio of the quenching rates, $k_q(R\text{-}S)/k_q(R\text{-}R)$, was 1.90. This demonstrates that the fluorescence quenching involved the contact of the molecules with a specific orientation. The enantioselective quenching ratio decreased as the solvent polarity increased. In acetonitrile, $k_q(R\text{-}S)/k_q(R\text{-}R)$ became 1.00, that is, no enantioselective response was detected. The fluorescence quenching rate was found to increase with the solvent polarity. A mechanism involving the competitive formation of an exciplex in nonpolar solvents and an electron-transfer ion pair in polar solvents was proposed to account for the solvent effects (Scheme 1). As shown in Scheme 1, the excited state of **27** encounters **1** to first form a loose complex (k_1). This complex may generate either a tight exciplex (k_2) or an electron-transfer ion pair (k_3). The ion pair in polar solvents should have a loose structure with no specific orientation required for **27** and **1**, leading to the diminished chiral discrimination. The quenching rate should also be faster in polar solvents than in nonpolar solvents.

The fluorescence quenching of **27** by the chiral amines **2** and **3** that contained more bulky alkyl substituents than that in **1** was further examined.[23] In *n*-hexane, the enantiomers of **2** quenched the

Scheme 1. A Proposed Mechanism for the Interaction of the Excited 27 with the Chiral Amine 1

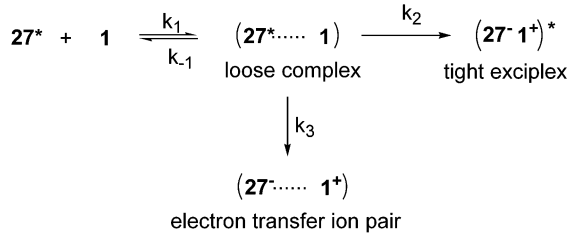

fluorescence of (*R*)-(−)-**27** with $k_q(R\text{-}S)/k_q(R\text{-}R)$ of 2.7. In the same solvent, the enantiomers of **3** gave $k_q(R\text{-}S)/k_q(R\text{-}R)$ of 4.0. Thus, the enantioselectivity increased as the size of the chiral quenchers increased. Similar to **1**, both **2** and **3** gave an enantiomeric quenching ratio of 1.00 in acetonitrile solutions. A significant increase in the enantioselectivity of the fluorescence quenching was observed when the temperature was decreased. At −10 °C, the $k_q(R\text{-}S)/k_q(R\text{-}R)$ was 2.9 for **1**, 4.7 for **2**, and 7.9 for **3**. Thus, lowering the temperature greatly enhanced the chiral discrimination in the fluorescence quenching.

The fluorescence of a 1,1′-binaphthyl compound anchored to a silica surface, **28**, was studied by Avnir et al.[24] When (*R*)-**28** was interacted with the enantiomers of the chiral amine **1** in a cyclohexane slurry, the ratio of the fluorescence quenching rates, $k_q(R\text{-}S)/k_q(R\text{-}R)$, was found to be 1.3. That is, the

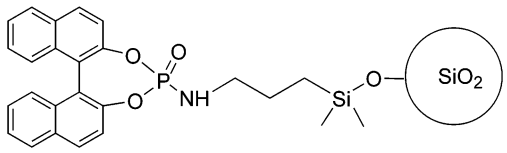

28

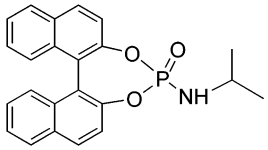

29

chiral silica surface was able to discriminate the enantiomers of the amine quencher. When (*S*)-**28** was used, $k_q(S\text{-}R)/k_q(S\text{-}S)$ was 1.2. Changing the solvent from cyclohexane to methanol caused the vanishing of the chiral recognition. This was the same as what was observed for the interaction of **27** with the chiral amines **1**−**3** when the solvent polarity was increased. No chiral discrimination was detected for the fluorescence of the homogeneous solution of **29** with the two enantiomers of **1** in toluene. The fluorescence quenching rate of **29** in the presence of **1** was about twice that of **28** by **1**. The diminished enantioselectivity of **29** was attributed to the flip-flop movements of its isopropylamine group. This movement was restricted in **28** as it was anchored to the surface of silica. The slower quenching rate of **28** by the amine than that of **29** was attributed to the shielding of one face of the binaphthyl rings by the silica surface which reduced its interaction with the amine.

In 1992, Iwanek and Mattay reported the fluorescence quenching of 1,1′-bi-2-naphthol (BINOL, **30**) by

a series of chiral amines (**1** and **4**−**7**).[25] The UV spectra of **30** in the presence of the amines in solvents such as benzene, ethyl ether, chloroform, ethyl acetate, tetrahedrofuran, and 1,2-dichloroethane showed red shifts for its long wavelength absorption, indicating the formation of hydrogen bond complexes. An additional peak appeared at about 360 nm in methanol or in the region of 360−400 nm in acetonitrile besides the one at 340 nm after **30** was treated with most of the amines. The stability constants for the BINOL−amine complexes in various solvents, determined by using the Benesi−Hildebrand method, were 0.16−98.8 dm^3 M^{-1}. The lowest was for **30** + **7** in THF and the highest for **30** + **5** in methanol. The lowest stability constants in THF could be attributed to the specific solvation of BINOL and amines by the basic THF oxygen through hydrogen bond formation. In cyclohexane and partly in other solvents, the stability constants indicated that the complexes of BINOL with primary amines were generally stronger than with tertiary amines. No chiral discrimination was observed for the ground state complexation.

The influence of chiral alcohols on the BINOL−amine complexes was measured. In the interactions of the acetonitrile solution of **30** + **5** with chiral alcohols **7**, **31**, and **32**, the two enantiomers of the amino alcohol **7** caused the biggest difference in the differential absorption spectra. Their stability

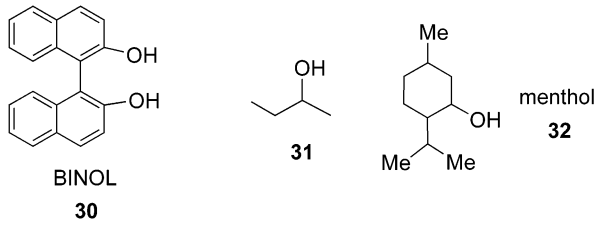

constant ratio, K[(*S*)-**30**+(*R*)-**5**+(−)-**7**]/K[(*S*)-**30**+(*R*)-**5**+(+)-**7**], was 1.21. The difference between the absorption spectra of (*S*)-**30** + (*R*)-**5** in the presence of the two enantiomers of **31** was small, but their stability constant ratio, K[(*S*)-**30**+(*R*)-**5**+(*R*)-**31**]/K[(*S*)-**30**+(*R*)-**5**+(*S*)-**31**], still gave a value of 1.16. Changing the solvent from acetonitrile to cyclohexane led to only a 2% difference in the stability constants. The stability constant difference for (+) and (−)-menthol (**32**) could not be obtained because (−)-**32** gave rise to very small and irregular changes in the absorption spectra.

The fluorescence spectra of the optically active BINOL **30** in the presence of the enantiomers of the chiral amines in various solvents were studied. In acetonitrile, BINOL gave absorption λ_{max} at 334 nm and emission λ_{max} at 359 nm. The amines (0.039−0.31 M) quenched the fluorescence of BINOL (6×10^{-5} M) at 350−450 nm. The Stern−Volmer constants decreased as the dielectric constants of the solvents increased for the primary amines. The fluorescence quenching of BINOL by the primary amines may involve a static quenching in cyclohexane because of the formation of a strong complex. The ratios of the Stern−Volmer constants for (*S*)-**30** and (*R*)-**30** in the presence of the optically active amines were ca. 0.89−1.16 with the enantioselective responses observed only in acetonitrile. This may be due to the formation of the charge separated excited ionic pairs, [**30**$^-$···H−NR_3^+]*, in acetonitrile. The small steric effect in the ground state hydrogen bond complexes might become larger in the excited state because of the orbital interactions in the excited ionic pairs. In the fluorescence quenching of BINOL by all the amines, a very weak emission at 450−640 nm grew with increasing amine concentration in all solvents and the strongest was observed in acetonitrile. This was attributed to the emission of the excited ionic pairs. The low enantioselectivity (the highest at 16%) in the fluorescence quenching of BINOL by the amines was because only a portion of the excited BINOL molecules was quenched by the formation of the excited ionic pairs, and most of them were quenched by a radiationless decay of the hydrogen bonded excited molecules.

Scheme 2. Photochemical Reaction of BINOL with Amines

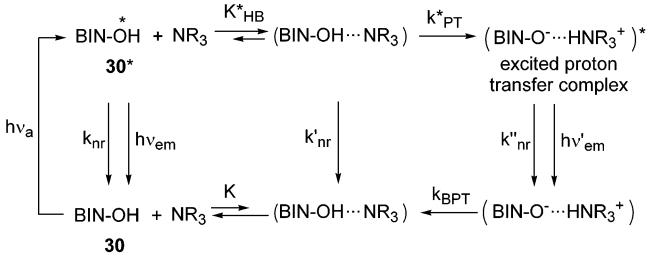

Scheme 2 summarizes the reaction of BINOL with amines. In this scheme, k_{nr}, k'_{nr}, and k''_{nr} are the rate constants for the nonradiative decay of the excited molecules and complexes; $h\nu_{em}$ and $h\nu'_{em}$ are the fluorescence emission of the excited BINOL and ion pairs; k^*_{PT} and k_{BPT} are the rate constants for the excited proton transfer and the ground state back proton transfer, respectively; K and K^*_{HB} are the equilibrium constants for the formation of the ground state hydrogen bonded complex and the excited state hydrogen bonded complex, respectively.

Townshend and co-workers found that the effective Stern−Volmer quenching constants of (*R*)- or (*S*)-**30** (8×10^{-6} M) in the presence of the chiral amine **4** (0−1.35×10^{-2} M) in acetonitrile solution were linear with the enantiomeric composition of **4**.[26] Addition of **4** to **30** decreased the intensity of the excitation maximum (λ_{exc} = 330 nm) and the emission maximum (λ_{emi} = 360 nm), but did not change the wavelengths. The Stern−Volmer constant of (*R*)-**30** + (*R*)-**4** was found to be very close to that of (*S*)-**30** + (*S*)-**4**, and that of (*R*)-**30** + (*S*)-**4** very close to that of (*S*)-**30** + (*R*)-**4**, indicating the role of chirality in the fluorescence quenching.

The chiral amine **4** could also quench the fluorescence of 2,2′-diamino-1,1′-binaphthyl (BINAM, **33**).[27] Compound **33** gave an emission maximum at 405 nm when excited at 350 nm in acetonitrile. The Stern−Volmer plots of (*R*)-**33** (6×10^{-6} M) in the presence of (*R*)- and (*S*)-**4** (0−1.3×10^{-2} M) showed a small but measurable enantioselective response. It was found that (*S*)-**4** quenched BINOL (*R*)-**30** more efficiently than (*R*)-**4**, whereas (*R*)-**4** quenched BINAM (*R*)-**33** more efficiently than (*S*)-**4**. Using the two fluorophores BINOL (*R*)-**30** and BINAM (*R*)-**33** could

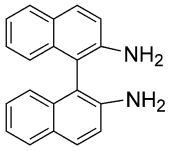

BINAM
33

determine the concentration of each enantiomer of **4** in an enantiomeric mixture. The following Stern−Volmer equation for two quencher systems was utilized: $I_0/I = 1 + K_{SV1}[Q_1] + K_{SV2}[Q_2]$. $[Q_1]$ and $[Q_2]$ are the concentrations of the two enantiomers of the amine quencher. The Stern−Volmer constants K_{SV1} and K_{SV2} for each enantiomer of the quencher with the two fluorophores were determined by using the pure enantiomers of the quencher and of the fluorophore. Although this method shows the potential of the 1,1′-binaphthyl compounds in determining the enantiomeric composition of chiral amines, the enantioselectivity is quite low.

The binaphthyl compounds **34** and **35** that contained boron−dipyrromethene fluorophores were studied by Beer et al.[28] They found that the fluorescence of **34** (5×10^{-6} M in acetonitrile, $\lambda_{emi} = 542$ nm) was significantly quenched by diisopropylethylamine. The

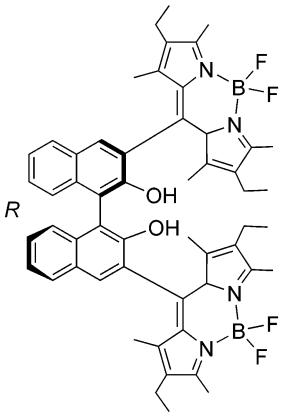

34

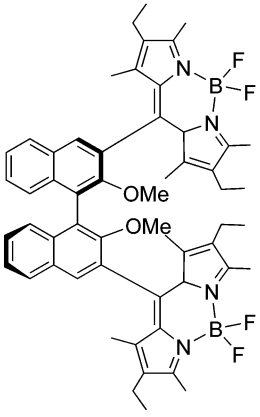

35

time-resolved experiments indicated that this was a static quenching process due to the formation of a nonfluorescent deprotonated species. The fluorescence lifetime of **34** was 5.15 ns, which did not change with the increasing concentration of the amine ($0-9 \times 10^{-5}$ M). Only at the high concentration of the amine ($>10^{-2}$ M) was there dynamic quenching of **34** observed which gave decreased fluorescence lifetime. The fluorescence of **35** could not be quenched by diisopropylethylamine. Even at high concentrations of the amine ($>10^{-2}$ M), there was only slight reduction in the fluorescence intensity of **35** due to dynamic quenching. These observations demonstrated that the interaction of the acidic hydrogens of **34** with the amine was very important for the fluorescence quenching. The Stern−Volmer constant for **34** and diisopropylethylamine was 1.1×10^4 M. It also represented the association constant since the static quenching dominated. The fluorescence spectra of **34** in the presence of the chiral amine (*R*)- and (*S*)-**4** were studied. It was found that the static

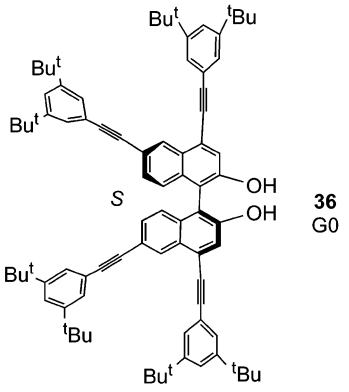

36
G0

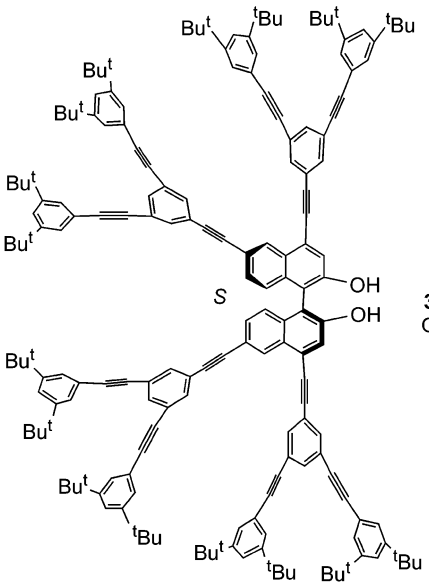

37
G1

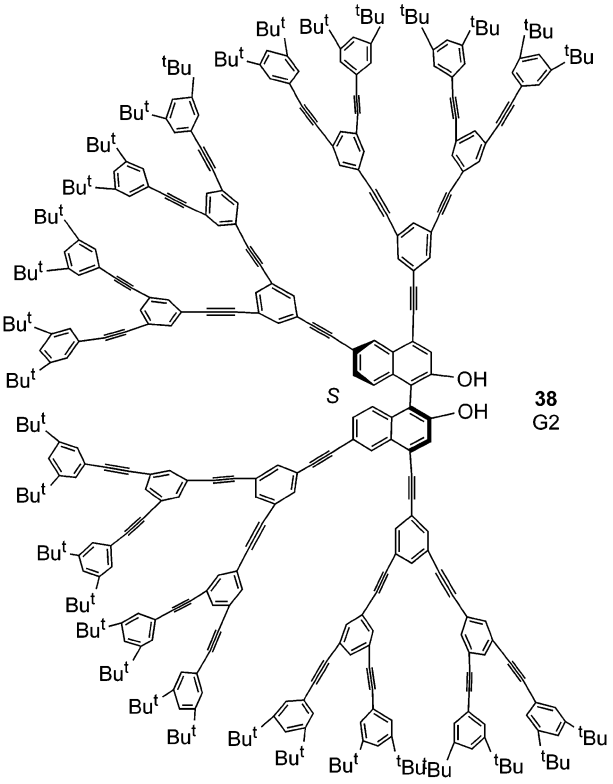

38
G2

quenching constants were $K_{SV} = 226\ M^{-1}$ for (*S*)-**4** and $K_{SV} = 161\ M^{-1}$ for (*R*)-**4**. Thus, the enantioselectivity was $K_{SV}(R\text{-}S)/K_{SV}(R\text{-}R) = 1.40$.

2.1.2. Binaphthyl Dendrimers

Pu and co-workers synthesized the 1,1′-binaphthyl dendrimers **36**−**38** that contained an (*S*)-BINOL core and phenyleneethynylene dendrons.[29,30] The UV absorption spectra of these dendrimers displayed two bands in methylene chloride with one strong band around 250−330 nm and a weak one around 340−400 nm. The strong band was attributed to the absorption of both the phenyleneethynylene dendrons and the binaphthyl core, and the weak one was due to the extended conjugation of the 4,4′,6,6′-tetraphenylethynyl-1,1′-bi-2-naphthol core. A large increase in absorption was observed in the band of 250−330 nm as the dendritic generation increased. In the meantime, the absorption band due to the core remained almost unchanged. The generation 2 (G2) dendrimer **38** showed 9-fold increases in the molar extinction coefficient at ca. 310 nm from the generation 0 (G0) dendrimer **36** due to the increased number of the diphenylethyne units. However, almost no shift in the absorption wavelength was observed because the *m*-phenylene linkage of the dendritic arms did not change the conjugation of the dendrimers.

Upon excitation at 310 nm where the phenyleneethynylene dendrons absorbed, the emission intensity at ca. 422 nm grew 12 times from the G0 dendrimer **36** to the G2 dendrimer **38**. No emission due to the dendrons **39** and **40** was observed in the fluorescence spectra of **37** and **38**. Thus, the light energy absorbed

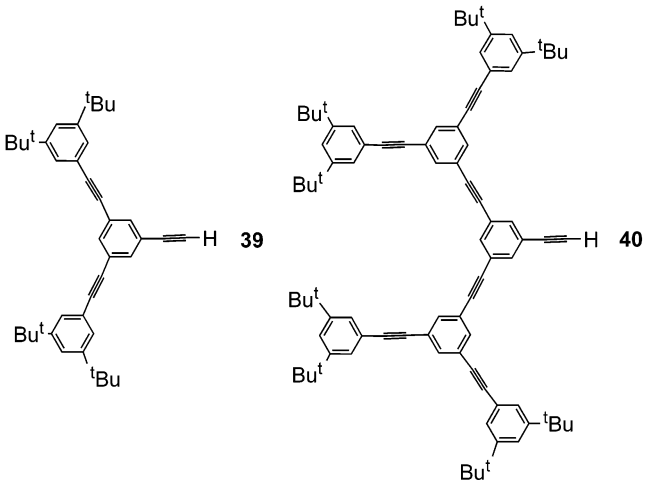

by the dendrons was effectively transferred to the core, giving the light-harvesting emission. The excitation spectra of the dendrimers also exhibited a large increase for the absorption at 310 nm from **36** to **38** when observed at 422 nm. The quantum yields of the G0, G1, and G2 dendrimers were found to be approximately 0.30, 0.32, and 0.40, respectively.

The fluorescence of the chiral dendrimer **38** was much stronger than that of BINOL. At 4.0×10^{-8} M in methylene chloride, while the fluorescence intensity of BINOL was close to the baseline, the signal of the dendrimer was very strong. Therefore, the dendrimer should be a much more sensitive sensor when used to interact with a fluorescence quencher.

The chiral amino alcohols including 2-amino-3-methyl-1-butanol (**8**), 2-amino-4-methyl-1-pentanol (**9**), and 2-amino-3-phenyl-1-propanol (**10**) were found to efficiently quench the fluorescence of the dendrimers. The fluorescence quenching followed the Stern−Volmer equation. As the dendrimer generation increased, the Stern−Volmer constants also increased. The higher generation dendrimers exhibited much greater reduction in fluorescence intensity than the lower generation one when treated with the amino alcohol quenchers. Thus, the dendritic branches significantly increased the fluorescent sensitivity.

The fluorescence quenching by the chiral amino alcohols was also found to be enantioselective. Under the same conditions, the (*S*)-enantiomer of the amino alcohols quenched the fluorescence of the (*S*)-dendrimers more efficiently than the (*R*)-enantiomer. The highest Stern−Volmer constant ratio was $K_{SV}(S)/K_{SV}(R) = 1.27$. Fluorescence quenching of the (*R*)-dendrimers by the chiral amino alcohols gave a mirror image relationship with that of the (*S*)-dendrimers which confirmed the enantioselective response. The effective Stern−Volmer constants of dendrimer **38** (4.0×10^{-8} M in 20:80 benzene:hexane) were linear with the enantiomeric composition of the amino alcohol **10**. This allowed the determination of the enantiomeric composition of the amino alcohol by measuring the fluorescence intensity of the chiral dendrimer.

In the absence of a quencher, the fluorescence lifetime of **38** was determined to be 1.6 ± 0.2 ns. Addition of the amino alcohol **10** at various concentrations caused little change in the fluorescence lifetime. Thus, only static quenching occurred in the interaction of **38** with the amino alcohol. Formation of nonfluorescent ground state hydrogen bond complexes between the hydroxyl groups of the dendrimer core and the amino alcohol was proposed to be responsible for the fluorescence quenching. Addition of NaOH to both the dendrimer and (*S*)-BINOL generated a new peak in the UV−vis spectra ca. 50 nm to the red of the lowest absorption maximum because of deprotonation. However, there was only a slight difference from their original UV absorption spectra when the dendrimers were treated with the amino alcohol **10**. This indicated that the dendrimer core could not be deprotonated by the amino alcohol and only a hydrogen bond complex formed. When the two hydroxyl groups of (*S*)-**38** were replaced with methoxyls, no quenching by an amino alcohol was observed.

Because of the static quenching mechanism, the observed K_{SV}'s (43−561 M^{-1}) should be the ground state association constants between the dendrimers and the amino alcohols. The K_{SV}'s increased as the solvent polarity decreased from methylene chloride to benzene/hexane. This was attributed to a stronger ground state hydrogen bonding interaction between the BINOL core and amino alcohols in the less polar solvent. The higher generation dendrimers also showed higher association constants with the amino alcohols.

Phenylene-based chiral binaphthyl dendrimers **41**−**43** were prepared.[31] Similar to dendrimers **36**−**38**, dendrimers **41**−**43** gave two major absorption bands

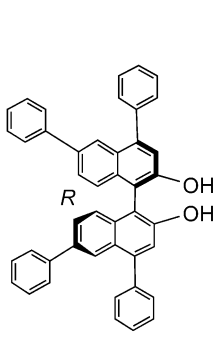

41

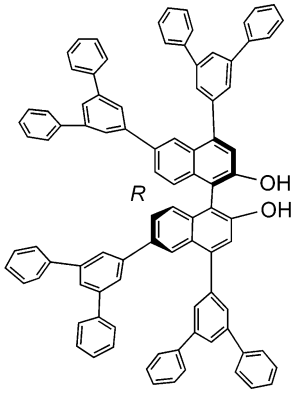

42

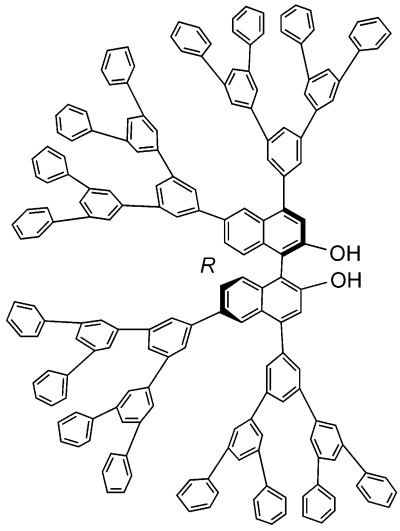

43

in their UV spectra at 250−300 nm and 300−370 nm. The shorter wavelength absorption increased significantly as the dendrimer generation grew. It was attributed to the absorption of both the phenylene dendrons and the binaphthyl moieties. No significant change in the second band was observed as the dendrimer generation increased. The long wavelength band was assigned to the absorption of the conjugated 4,4′,6,6′-tetraphenyl-1,1′-bi-2-naphthol core. These dendrimers showed emissions at 395−405 nm when excited at 256 nm where the absorption was mostly due to the benzene units of the dendrons. From the G0 dendrimer **41** to the G2 dendrimer **43**, the fluorescence intensity increased about 7.5 times at the same molar concentration. The emission of the dendritic phenylene branches was not observed in the fluorescence spectra of the dendrimers. Thus, there was an efficient energy migration from the dendritic light absorbing antenna to the more conjugated core. This light harvesting effect greatly enhanced the fluorescence of the higher generation dendrimers. The efficient intramolecular energy migration was supported by their excitation spectra. A large increase for the excitation maximum at 256 nm from the G0 dendrimer **41** to the G1 **42** and the G2 **43** appeared while observed at 405 nm. The fluorescence intensity of the dendrimers was also much stronger than that of BINOL.

When the G2 dendrimer **43** was treated with 2-amino-1-propanol (**11**) in methylene chloride solution, no significant fluorescent quenching was observed. However, with the addition of hexane as the cosolvent, the amino alcohol efficiently quenched the fluorescence of the dendrimer. A less polar solvent might have provided a better environment for the hydrogen bonding interaction between the hydroxyl groups of the dendrimer and the amino alcohol. The fluorescence quenching of (*R*)-**43** (1.0×10^{-7} M) by the optically pure amino alcohol (*R*)- and (*S*)-**11** (2.0×10^{-3} to 6×10^{-3} M) obeyed the Stern−Volmer equation with $K_{SV}(R) = 243.5\ M^{-1}$ and $K_{SV}(S) = 216.0\ M^{-1}$. Therefore, the fluorescence quenching of **43** by the amino alcohol was enantioselective with $K_{SV}(R)/K_{SV}(S) = 1.13$. The (*R*)-enantiomer of the amino alcohol quenched the fluorescence of the (*R*)-dendrimer more efficiently than the (*S*)-enantiomer. The fluorescence quenching of the G0 dendrimer and the G1 dendrimer by (*R*)- and (*S*)-**11** gave $K_{SV}(R) = 75.5\ M^{-1}$ and $K_{SV}(S) = 63.5\ M^{-1}$ for **41**, and $K_{SV}(R) = 99.9\ M^{-1}$ and $K_{SV}(S) = 88.4\ M^{-1}$ for **42**. The fluorescence quenching of dendrimer **43** in the presence of other amino alcohols such as leucinol (**9**) and 2-amino-3-methyl-butanol (**8**) was also enantioselective with $K_{SV}(R)/K_{SV}(S)$ in the range of 1.09−1.18. The higher generation dendrimers displayed greater fluorescence intensity change and were much more sensitive sensors toward the chiral quenchers.

2.1.3. Oligomeric and Polymeric Binaphthyls

Interaction of the dimeric binaphthyl compound **44** and its polymer **45** with the chiral amines **4** and **12** was investigated by Wang et al.[32] The ^{1}H NMR spectrum of **44** with (*R*)- or (*S*)-**4** in $CDCl_3$ exhibited

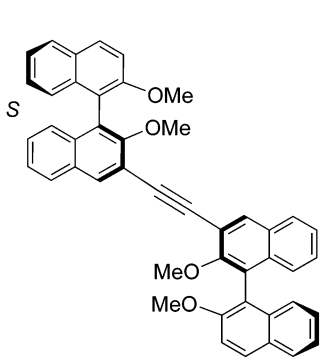

44

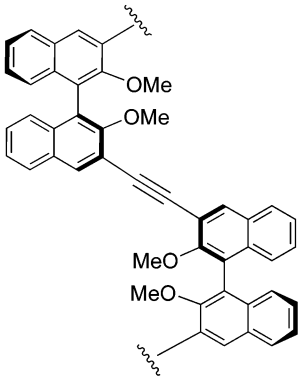

45

chiral discrimination in binding. The fluorescence spectra of **44** and **45** (1.0×10^{-5} M in acetonitrile, $\lambda_{emi} = 410$ nm) in the presence of (*R*)-/(*S*)-**4** and (*R*)-/(*S*)-**12** (0 to $<2.5 \times 10^{-4}$ M) were studied. It was found that the fluorescence intensity of **44** and **45** responded differently to the two enantiomers of **4** or **12** but the observed quantum yield data were scattered with respected to the concentration of the amines.

Binaphthyl dimers **46** and **47** were treated with the chiral amines **4** and **13**.[33] Both ^{1}H NMR and UV absorption spectra showed chiral discrimination in the binding of **46** or **47** with (+)-/(−)-**4** or (+)-/(−)-

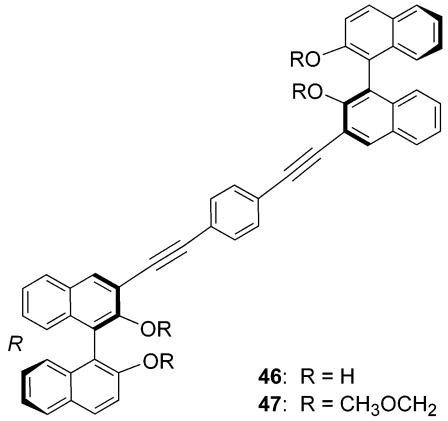

13. The UV titration experiments supported the formation of 1:1 complexes between the binaphthyl hosts and the amine guests. In methylene chloride solutions, the association constant ratio $K(-)/K(+)$ was 3.8:1 (158.7/41.7) for the interaction of **46** with (−)-**4** and (+)-**4**; 1:3.0 (20.4/60.2) for **46** with (−)-**13** and (+)-**13**; 3.8:1 (471.7/125.0) for **47** with (−)-**4** and (+)-**4**; and 1:2.5 (45.0/112.5) for **47** with (−)-**13** and (+)-**13**. It is unclear why the association constant of the hydroxyl group protected **47** with an amine was greater than that of the unprotected **46** with the same amine. The fluorescence spectra of **46** and **47** (1.4×10^{-5} M in acetonitrile, $\lambda_{emi} = 410$ nm) in the presence of (+)-/(−)-**4** and (+)-/(−)-**13** (0 to $<7 \times 10^{-4}$ M) were studied. The fluorescence intensity of **46** and **47** responded differently to the two enantiomers of **4** or **13**. The observed quantum yields were scattered with both decreasing and increasing depending upon a specific concentration of the amines.

Lin and co-workers synthesized the oligomeric 1,1′-bi-2-naphthol **48a**−**d**.[34] The UV absorption wavelengths of these oligomers were found to be similar to those of [(*R*)-BINOL, (*R*)-**30**] but with greatly

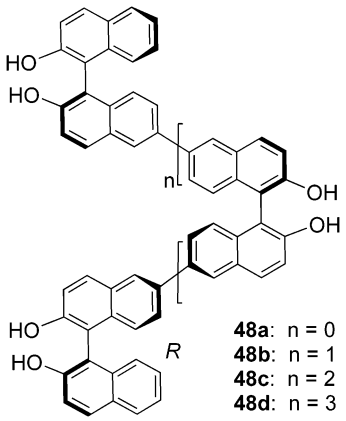

increased extinction coefficients (up to 40-fold increases for the long wavelength absorption). The fluorescence spectra of these 1,1′-binaphthyl oligomers **48a**−**d** (5.0×10^{-7} M in acetonitrile) gave almost identical emissions with two major peaks around 380 and 395 nm ($\lambda_{exc} = 325$ nm). The fluorescence intensity increased from **48a** to **48c** and then decreased from **48c** to **48d**. The quantum yields decreased from **48a** (0.50) to **48d** (0.21), and the quantum yield of (*R*)-BINOL was 0.1. Interaction of (*S*,*S*,*S*)-**48b** (5.0×10^{-7} M) with 1,2-diaminocyclohexane (*R*,*R*)-**14** and (*S*,*S*)-**14** (0 to $<4 \times 10^{-4}$ M) in a mixed solvent of bezene:hexane (20:80) was studied. An enantioselective fluorescent quenching was observed with $K_{SV}(SS) = 10446$ M^{-1} for (*S*,*S*,*S*)-**48b** + (*S*,*S*)-**14**, and $K_{SV}(RR) = 12611$ M^{-1} for (*S*,*S*,*S*)-**48b** + (*R*,*R*)-**14**, i.e., $K_{SV}(SS)/K_{SV}(RR) = 0.83$. The enantioselective responses were confirmed by studying the interaction of (*RRR*)-**48b** with (*R*,*R*)-**14** and (*S*,*S*)-**14**.

Zhang and Pu synthesized the helical polybinaphthyl **49** (Chart 1) by treatment of polymer **50** with CF_3CO_2H at room temperature in methylene chloride.[35] Polymer **49** contained fused polyaromatic rings as the repeating units which forced it to adopt a propagating helical chain structure. It was completely soluble in common organic solvents such as THF, methylene chloride, and chloroform. Because of its dark color in solution, its specific optical rotation fluctuated at around −531 ($c = 0.1$, CH_2Cl_2), the opposite sign of that of polymer **50** {$[\alpha]_D = +36.8$ ($c = 0.1$, CH_2Cl_2)} with greatly increased value. GPC gave its molecular weight as $M_w = 17900$ and $M_n = 10500$ (PDI = 1.70). New absorptions at the long wavelength between 390 and 560 nm were observed after polymer **50** was converted to **49**. In the fluorescence spectra, a very large red shift ($\Delta\lambda = 123$ nm) was observed going from **50** ($\lambda_{emi} = 398$ nm) to **49** ($\lambda_{emi} = 521$ nm).

Polymer **49** was found to be a much more efficient fluorescent sensor than BINOL when interacting with an amino alcohol quencher. The fluorescence spectra of (*R*)-BINOL and **49** were compared at 1.0×10^{-5} M in CH_2Cl_2/hexane (1:1) for their interactions with (1*R*,2*S*)-(−)-*N*-methylephedrine (**7**, 3.0×10^{-2} M). The fluorescence intensity ratio I_0/I (I_0, without the amino alcohol; I, with the amino alcohol) was 1.3 for BINOL, but 3.4 for **49**. This significantly increased fluorescence sensitivity of the polymer over BINOL toward the amino alcohol might be due to an energy migration along the helical conjugated polymer chain. It could also be attributed to the lower $\pi-\pi^*$ band-gap of the polymer which may facilitate the photoinduced electron transfer quenching by the amino alcohol. The fluorescence quenching of **49** by the two enantiomers of **7** was also found to be different with an ef (ef = $|I_0 - I_{RS}|/|I_0 - I_{SR}|$, the enantiomeric fluorescence difference ratio) value of 1.12 ± 0.01. Although this enantioselectivity was small, it was larger than using (*R*)-BINOL which showed no difference at all in the fluorescence quenching when treated with the two enantiomers of the amino alcohol **7**.

2.1.4. Binaphthyl Macrocycles

Lee and Lin constructed the metallobinaphthyl macrocycle **51** by employing the self-assembly of the chiral binaphthyl ligand with a Re precursor.[36] This compound gave two emission peaks around 412 and

Chart 1

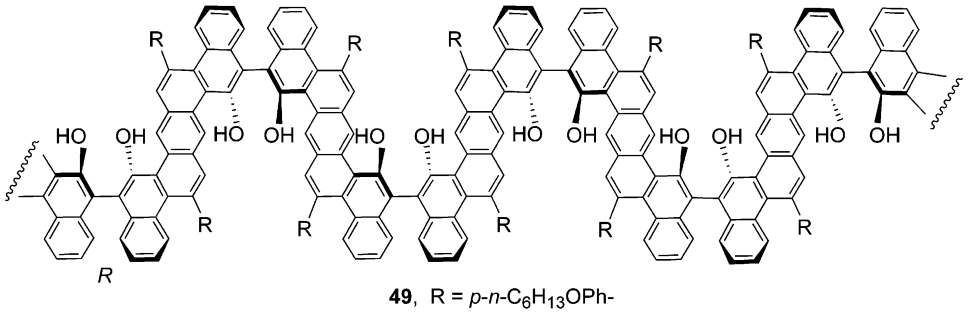

49, R = *p*-*n*-C_6H_{13}OPh-

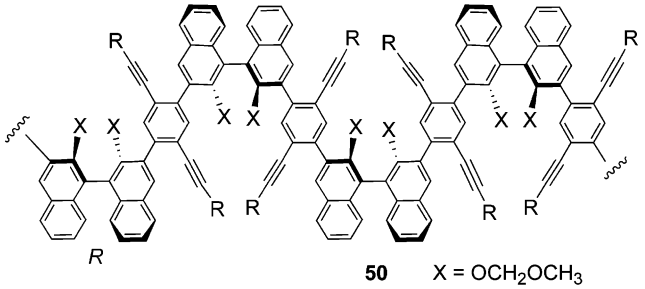

50 X = OCH_2OCH_3

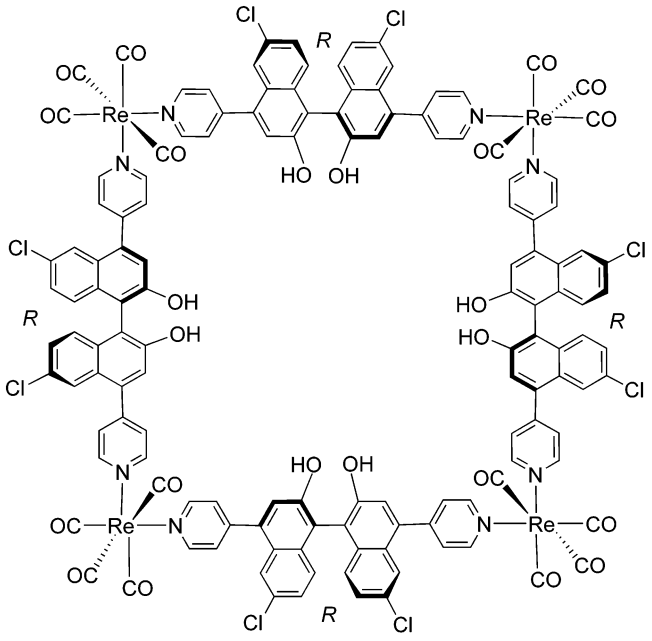

51

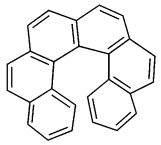

52

536 nm in THF when excited at 360 nm. The peak at 412 nm was assigned to the $\pi-\pi^*$ excited state of the ligands, and the weaker luminescence at 536 nm was attributed to a ^{3}MLCT excited state. The emission of **51** (2.2×10^{-6} M in THF) at 412 nm was quenched enantioselectively by 2-amino-1-propanol (**11**, 0 to <0.15 M) with $K_{SV}(S) = 7.35\ M^{-1}$ and $K_{SV}(R) = 6.02\ M^{-1}$, i.e., $K_{SV}(S)/K_{SV}(R) = 1.22$. When the hydroxyl groups of **51** were methylated, no enantioselectivity was observed in the fluorescent quenching.

2.2. Helicene Fluorophores

Raut and Tottertf studied the fluorescence of hexahelicene **52** in the presence of the chiral amine (*S*)-**15**.[37] Optically active **52** was obtained by flash chromatography of the racemic mixture on silica that was loaded with (+)-2-(2,4,5,7-tetranitro-9-fluorenylideneaminooxy)propionic acid [(+)-TAPA]. This process gave (+)-**52** (41% ee) and (−)-**52** (90% ee) for the fluorescent experiments. Aromatic amines readily quenched the fluorescence of **52** in acetonitrile but not aliphatic amines. This was probably due to the better $\pi-\pi$ interaction between **52** and the aromatic unit of the amines in the polar solvent.

The fluorescence quenching of racemic **52** and the optically active **52** by the optically active arylamine (*S*)-**15** in various solvents was investigated. It was found that the quenching constant was about the same in 1,2-dichloroethane and EtOH, but there was a factor of 7 increase in MeOH and another factor of 7 increase in acetonitrile. Helicene **52** could not be quenched by **15** in solvents such as *n*-hexane and dioxane. Negative enthalpies of activation of the quenching reaction in EtOH and MeOH were observed, indicating exciplex formation. Almost no chiral discrimination was observed in this system.

Reetz and Sostmann reported the use of the helicene diol **53** in fluorescent recognition.[38] The specific optical rotation of (+)-**53** was $[\alpha]_D = +2530$ ($c = 0.26$, CH_2Cl_2). It gave fluorescence maxima at 425, 445,

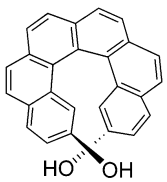

53

and 479 nm ($\lambda_{exc} = 318$ nm), and phosphorescence

signals in the range of 470−670 nm in methylene chloride solution. The fluorescence of **53** was quenched enantioselectively by the amines and amino alcohols **1**, **5**, **8**, **10**, **11**, and **16**−**18**. The fluorescence quenching followed the Stern−Volmer equation. The amino alcohol **11** showed the highest enantioselectivity with $K_{SV}(R)/K_{SV}(S) = 2.1$ (171/81). When the oxygen atoms of **53** were protected with alkyl groups, no chiral discrimination was observed. Thus, the enantioselective fluorescent response might require a hydrogen bonding interaction between the fluorophore and the quencher.

2.3. Calixarene Fluorophores

Diamond and co-workers reported the use of calixarenes to carry out the fluorescent determination of the enantiomeric composition of chiral amines.[39] Compound **54** is a calix[4]arene that contains macrocyclic oligomeric phenols. The authors prepared the calixarene derivatives **55**−**57** that contained chiral fluorophores for the fluorescent recognition of the chiral amine and amino alcohol molecules **4** and **19**.

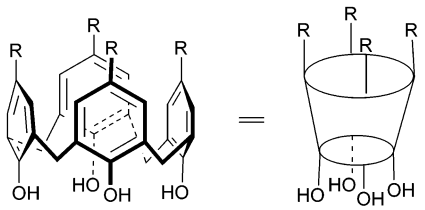

54

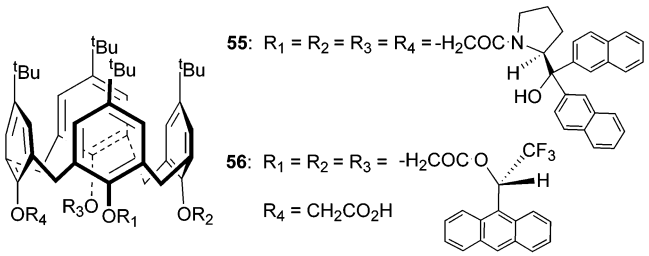

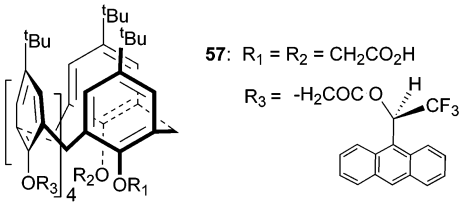

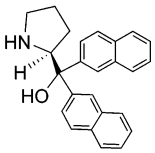

58

The fluorescence of **55** in chloroform at 337 nm ($\lambda_{exc} = 274$ nm) could be quenched by the chiral amine **4**. The fluorescence quenching of **55** (1×10^{-6} M) by racemic **4** in the concentration range of 0−13.5 mM followed the Stern−Volmer equation. Compounds **56** and **57** gave a maximum emission at 416 nm when excited at 258 nm. The fluorescence quenching of **56** and **57** (2×10^{-7} M) by racemic **4** (0−3 and 0−2.5 mM respectively) also followed the Stern−Volmer equation.

The (*R*)-enantiomer of **4** quenched the fluorescence of **55** much more efficiently than the (*S*)-enantiomer with $K_{SV}(R) = 0.052$ and $K_{SV}(S) = 0.028$, i.e., $K_{SV}(R)/K_{SV}(S) = 1.856$. It was observed that for **56** $K_{SV}(R) = 0.363$ and $K_{SV}(S) = 0.377$ [$K_{SV}(R)/K_{SV}(S) = 0.962$], and for **57** $K_{SV}(R) = 0.3485$ and $K_{SV}(S) = 0.3350$ [$K_{SV}(R)/K_{SV}(S) = 1.040$]. Thus, calixarene **55** showed significant enantioselective recognition of **4**, but **56** and **57** did not. The K_{SV} of **55** was found to be linear with the enantiomeric composition of **4**. When the chiral fluorophore **58** was interacted with the enantiomers of **4**, almost no enantioselectivity was observed. This indicated that the calixarene macrocycle was necessary for the chiral recognition. The fluorescence of compound **55** was also quenched by norephedrine **19** enantioselectively. With a known concentration, the enantiomeric compositions of **4** and **19** were determined by a single fluorescent measurement.

Compound **55** (5×10^{-7} M) was interacted with the amino alcohol **20** (0−3.75×10^{-3} M) in methanol.[40] Significant enantioselective fluorescent quenching was observed with $K_{SV}(R) = 0.054$ and $K_{SV}(S) = 0.133$ [$K_{SV}(R)/K_{SV}(S) = 2.463$].

2.4. Camphor Fluorophores

Fox and Singletary found that the fluorescence quenching of (+)- or (−)-camphor (**59**) at 420 nm ($\lambda_{exc} = 300$ nm) in hexane (3×10^{-2} M) by the chiral amines **1**, **4**, and **21**−**23** (0−0.3 M) followed the Stern−Volmer equation.[41] Both the responses of the

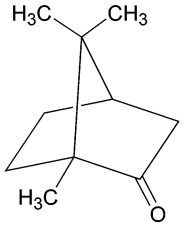

(1*R*)-(+)-Camphor

(*R*)-**59**

two enantiomers of camphor toward one enantiomer of a chiral amine and the responses of the two enantiomers of a chiral amine toward one enantiomer of camphor were investigated, but only very small enantioselectivity in the fluorescence quenching process was observed.

2.5. Pyrene Fluorophores

De Schryver and co-workers studied the fluorescence of *N*-acetyl-1-pyrenylalanine methyl ester (**60**) in the presence of the aromatic amine **24** and the aliphatic amine **1**.[42] The aromatic amine L-**24** (1×10^{-4} to 9×10^{-4} M in toluene) quenched the fluorescence of D- and L-**60** (10^{-5} M) at around 400 nm. In the meantime, it also gave rise to a new and broad long wavelength emission band above 500 nm. This new band was attributed to the emission of the exciplex of L-**24** with **60**. The excitation spectra showed that this long wavelength emission corresponded to the excitation of the pyrenyl at 378 nm.

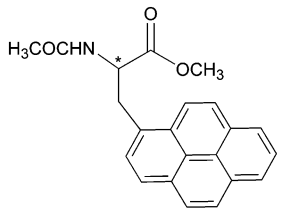

N-acetyl-1-pyrenylalanine methyl ester

60

The aliphatic amine (*S*)-**1** (0.6×10^{-2} to 4.8×10^{-2} M in isooctane) quenched the fluorescence of D- and L-**60** (10^{-5} M) very inefficiently, and the corresponding exciplex emission band was also very weak. More polar solvents led to more effective fluorescence quenching but no increase in the exciplex emission.

The fluorescence quenching rates of **60** by the two amines were found to be independent of the amine concentration. This indicated that there was no ground state interaction between the fluorophore and the quenchers. The chiral discrimination in the fluorescence quenching was too small to observe.

2.6. Using Crown Ethers

When the acridino crown ether **61** and the dimethyl acridino crown ether **62** were treated with the ammonium ions **25** and **26** in acetonitrile, Prodi et al. found that **61** and **62** bound **25** and **26** without the formation of the protonated acridinium ions as indicated by the UV absorption measurements.[43]

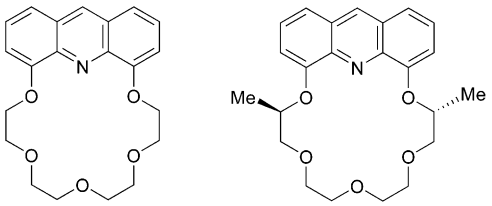

61 **62**

That is, the interaction of **61** or **62** with **25** and **26** was not simply acid−base reaction. When (*R*)-**25** or (*S*)-**25** was added to a solution of **61** or **62** in acetonitrile, the fluorescence intensity of the naphthalene unit ($\lambda_{emi} = 330$ upon excitation at 295 nm where both components absorb) was almost completely quenched at less than a 1:1 ratio of the ammonium and crown ether. In the meantime, the fluorescence of the acridine unit ($\lambda_{emi} = 440$ nm excited at 295 or 380 nm) was only partially quenched. The fluorescence quenching might have involved an electron transfer from the excited state of (*R*)-**25** or (*S*)-**25** to the acridine ring to form a nonemitting charge separated complex. The fluorescence quantum yields of **62** in the presence of either (*R*)-**25** or (*S*)-**25** were found to be identical ($\Phi_{\mathbf{62}+(R)-\text{or}(S)-\mathbf{25}} = 0.066$ and $\Phi_{\mathbf{62}} = 0.10$). However, the association constants of the two enantiomers with the crown ether, obtained by measuring the fluorescence intensity of the acridine at 445 nm and that of the ammonium salt at 330 nm, exhibited large differences with 4.4×10^5 M^{-1} for **62** + (*R*)-**25** and 2.3×10^6 M^{-1} for **62** + (*S*)-**25**. The ammonium salts (*R*)-**26** and (*S*)-**26** also gave very different association constants when complexing with **62**, i.e., 3.4×10^5 M^{-1} for **62** + (*R*)-**26** and 1.7×10^6 M^{-1} for **62** + (*S*)-**26**. When **62** was treated with (*R*)-**26** or (*S*)-**26**, a modest fluorescence increase of the acridine was observed with $\Phi_{\mathbf{62}+(R)-\text{or}(S)-\mathbf{26}} = 0.11$.

3. Enantioselective Fluorescent Recognition of Amino Acids and Derivatives

Fluorescent recognition of amino acids involves the use of the amine-based 1,1′-binaphthyl macrocycles to interact with the acid functions, the crown ether-based fluorophores to bind the ammonium salts, and the competitive binding of amino acids with cyclodextrins equipped with both a fluorophore and a metal coordination site. Proteins and enzymes have also been used to recognize amino acids that were covalently bound with a fluorophore such as a dansyl, a carbazole, and a pyrenyl. These studies were conducted in either aqueous solutions or organic solvents. Although the scope of the research on the enantioselective fluorescent recognition of amino acids is still quite limited, high enantioselectivity has been achieved in certain cases.

3.1. Using 1,1′-Binaphthyls

Pu and co-workers investigated the use of the chiral bisbinaphthyl macrocycle **63** in the fluorescent recognition of amino acid derivatives.[44−46] When a benzene solution (containing 2% DME = dimethoxyethylene) of (−)-**63** was excited at 340 nm, it exhibited two emission maximums at 365 (λ_{short}) and 424 (λ_{long}) nm. DME was added to improve the solubility of the highly polar amino acid derivatives in the fluorescent measurements. Both (−)-**63** and (+)-**63** were used to recognize the N-protected amino acids **64**−**70** (Figure 2).[46a]

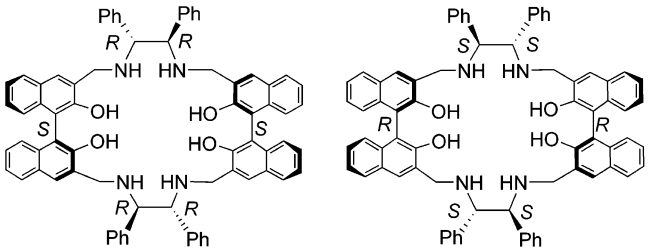

(-)-**63** (+)-**63**

When (+)-**63** was treated with D- or L-**64**, significant fluorescence enhancement especially at λ_{long} was observed. The enantiomer D-**64** enhanced the long wavelength emission 5.7 times more than L-**64** did, i.e., ef = 5.7 [ef: enantiomeric fluorescence difference ratio = $(I_D - I_0)/(I_L - I_0)$]. The fluorescence measurements demonstrated that the fluorescence of (+)-**63** increased over 4-fold with the increasing concentration of D-**64**, but only a small increase for the fluorescence of (+)-**63** by L-**64** was observed.

The interaction of (−)-**63**, the enantiomer of (+)-**63**, with D- and L-**64** showed that L-**64** caused much greater fluorescence enhancement for the emission of (−)-**63** at the long wavelength than D-**64**. This confirmed the enantioselective response of (+)- or (−)-**63** toward the enantiomers of the amino acid **64**.

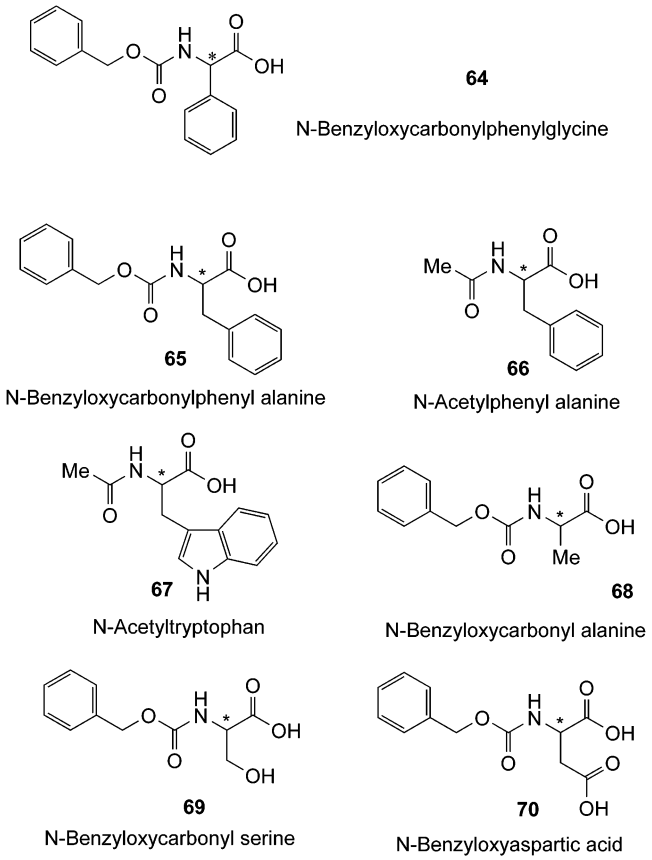

Figure 2. Structures of the N-protected amino acids **64**−**70**.

The ^{1}H NMR spectra of (−)-**63** and L-**64** in a variety of ratios in benzene-d_6 at a constant total concentration of 4.0×10^{-3} M gave the Job plot of $\Delta\delta X$ versus the mole fraction (X) of L-**64**. A maximum at $X = 0.8$ was observed which indicated the formation a 1:4 complex for (−)-**63** and L-**64** under the conditions. Probably all four nitrogen atoms of (−)-**63** were interacting with the acidic protons of four L-**64**. Other binding modes might also exist as a shoulder was observed in the Job plot. In the bisbinaphthyl macrocycle, its nitrogen atoms were expected to quench the fluorescence of the naphthyl fluorophores by the PET process. Interaction of these nitrogen atoms with the acidic proton of L-**64** made their lone pair electrons unavailable for PET, leading to the observed large fluorescence enhancement. The fluorescence experiments demonstrated that L-**64** should bind (−)-**63** more strongly than D-**64**. In the same way, D-**64** should also bind (+)-**63** more strongly than L-**64**.

The fluorescence intensity change of (+)-**63** with respect to the enantiomeric composition of **64** was studied. The fluorescence intensity of (+)-**63** increased linearly with the increasing D-component of the amino acid. Thus, the chiral bisbinaphthyl macrocycle could be used as a fluorescent sensor to readily determine the enantiomeric composition of this amino acid.

The interactions of (−)-**63** with other N-protected amino acids **65**−**70** besides **64** were also examined (Figure 2). Table 1 summarizes the highest ef's observed when (+)- or (−)-**63** was treated with the two enantiomers of these amino acid derivatives. All of these compounds enhanced the fluorescence of the binaphthyl fluorophore. Various degrees of enantioselectivity were observed. As shown in Table 1, when the benzyloxycarbonyl protecting group of **65** was replaced with the acetyl group of **66**, the enantioselectivity was inverted. Amino acids **67**, **68**, and **70** also showed the opposite enantioselectivity to that of **64**. The additional hydroxyl or carboxylic acid group of **69** and **70** gave a greatly reduced enantioselective fluorescent response. In Table 1, different amounts of DME were used because of the different solubility of the substrates. The amount of DME in the solution was also found to affect the fluorescence spectrum of **63**.

Table 1. Results for the Enantioselective Fluorescent Responses of (+)- or (−)-63 to the Amino Acids 64−70

amino acid	solvent	concn (M)	*ef*
64	C_6H_6/2%DME	4×10^{-3}	5.7[a,c]
65	C_6H_6/2%DME	2×10^{-3}	1.9[a,c]
66	C_6H_6/20%DME	2×10^{-2}	1.7[b,c]
67	C_6H_6/12%DME	4×10^{-3}	2.2[a,d]
68	C_6H_6/0.1%DME	2×10^{-3}	1.7[a,d]
69	C_6H_6/8%DME	2×10^{-2}	1.2[a,c]
70	C_6H_6/4%DME	5×10^{-3}	1.1[a,d]

[a] Using (+)-**63** (1.0×10^{-4} M). [b] Using (−)-**63** (1.0×10^{-4} M). [c] D/L. [d] L/D.

The 6,6′-substituted bisbinaphthyl compounds **71** and **72** were prepared.[46b] Introduction of the 6,6′-conjugated substituents to the binaphthyl compounds not only caused red shifts for the emission maxima but also enhanced the fluorescence intensity by about 2 orders of magnitude. The 6,6′-substituted macrocycles **71** and **72** gave intense long wavelength emissions at 445 and 491 nm, respectively, when excited at 305 nm. They also gave short wavelength emissions at 379 and 403 nm, respectively. The fluorescence responses of **71** and **72** to D- and L-**64** were investigated. The chiral amino acid quenched the long wavelength emissions of both macrocycles but enhanced their short wavelength emissions. Both

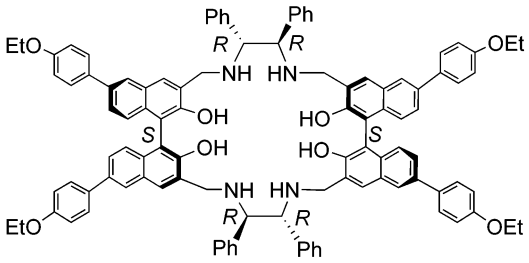

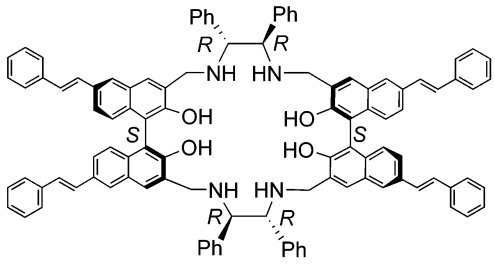

macrocycles exhibited very high enantioselectivity in their fluorescent responses to the amino acid. The observed ef values were up to 10. These compounds are useful as highly sensitive as well as enantioselective fluorescent sensors for the recognition of the amino acids.

Yanagida and co-workers capped the surface of ZnO nanocrystallites with (*R*)- or (*S*)-1,1′-binaphthyl-2,2′-diylhydrogen phosphate (**73**) which were then used as fluorescent sensors for the recognition of D- and L-tryptophan (**74**).[47] Hexagonal ZnO nanocrystallites with a mean diameter of 4.4 nm were obtained by heating $Zn(OAc)_2 \cdot 2H_2O$ in ethanol followed by the addition of $LiOH \cdot H_2O$ in an ultrasonic bath. The solution of the ZnO nanocrystallites in methanol displayed a steep absorption onset at 360 nm and an absorption peak at 330 nm. Its emission was observed at 550 nm. Addition of 50 μL of a methanol solution of (*R*)- or (*S*)-**73** to 50 mL of a methanol solution of the ZnO nanocrystallites (5 mM) gave the 1,1′-binaphthyl-capped materials. Chemical binding through the phosphate anion to the surface zinc atoms was supported by NMR and IR studies. The SiO_2 nanocrystallites capped with (*R*)- and (*S*)-1,1′-binaphthyl-2,2′-diamine (**75**) were also prepared. The binding in these materials was probably due to electrostatic interaction between the cationic group derived from **75** (protonation) and the negatively charged surface of SiO_2.

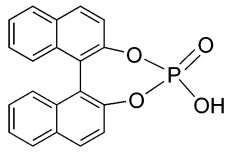

73

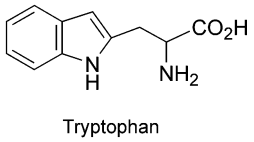

Tryptophan

74

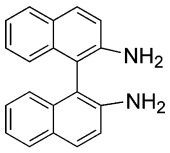

75

Compound **73** in methanol exhibited an emission maximum at 365 nm when excited at 230 or 290 nm. For the **73**−ZnO in methanol, excitation at 350 nm led to the emission of the ZnO nanocrystallites. Addition of D- and L-**74** to **73**−ZnO led to the fluorescence quenching of ZnO at 550 nm probably due to electron transfer from tryptophan to the excited ZnO. A small chiral discrimination was observed. D-Tryptophan quenched the fluorescence of (*R*)-**77**−ZnO slightly more effectively than L-tryptophan ($I_L/I_D < 1.04$). The opposite effect was observed when (*S*)-**73**−ZnO was interacted with D- and L-tryptophan. Increase in chiral discrimination was observed when the molar ratio of (*R*)- or (*S*)-**73** to ZnO increased from 0.01 to 0.05 ($I_L/I_D = 1.08$). The chiral discrimination then started to decrease with further increasing of the coverage of ZnO by **73**. No chiral discrimination was observed when D- and L-tryptophan were used to quench ZnO bounded with racemic **73**.

D- and L-Tryptophan also quenched the emission of **73** at 365 nm on the surface of ZnO with small chiral discrimination ($I_L/I_D < 1.06$). L-Tryptophan quenched the emission of (*R*)-**73**−ZnO slightly more effectively than D-tryptophan. No chiral discrimination was observed when D- or L-tryptophan interacted with free (*R*)- or (*S*)-**73** molecules. Thus, the organization of **73** on the surface of the nanocrystallite contributed to the observed chiral responses.

Small chiral discrimination was observed when D- and L-tryptophan were used to quench the emission of **75** in the (*R*)- and (*S*)-**75**-capped SiO_2 nanocrystallites. The fluorescence quenching of (*R*)-**75**−SiO_2 by L-tryptophan and (*S*)-**75**−SiO_2 by D-tryptophan was more efficient than (*R*)-**75**−SiO_2 by D-tryptophan and (*S*)-**75**−SiO_2 by L-tryptophan. The values of the I_L/I_D (<1.03) were smaller than those of (*R*)- and (*S*)-**73**−ZnO. No chiral discrimination was observed when D- and L-tryptophan were used to interact with either the racemic **75** capped SiO_2 or the free **75** molecules.

3.2. Using Crown Ethers

In 1980, Tundo and Fendler reported the use of the chiral crown ethers **76a**−**c** and **77a**−**c** in the fluorescent recognition of amino acid derivatives.[48] Compounds **76a**,**b** and **77a**,**b** contained a tryptophan unit as the fluorophore, and compounds **76c** and **77c** contained pyrene as the fluorophore. The absorption spectra of **76a**,**b** and **77a**,**b** were identical in methanol, but a small difference in the emission intensity

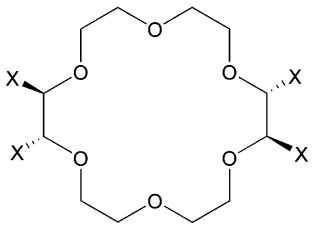

76

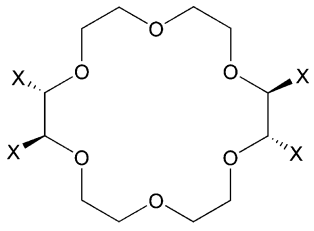

77

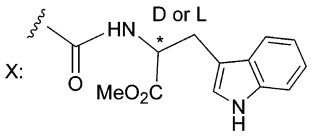

D: **76a**, **77a**
L: **76b**, **77b**

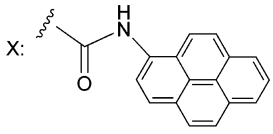

76c
77c

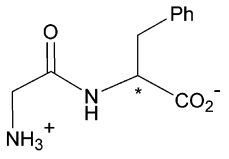

78

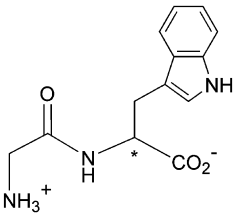

79

was observed for these diastereomers with $\Phi_{\mathbf{76b}} = 0.18$ and $\Phi_{\mathbf{77b}} = 0.20$. The crown ether **77b** ($\lambda_{emi} = 350$ nm and $\lambda_{exc} = 290$ nm) showed only a modest chiral recognition in the fluorescence quenching by glycine-L-phenylalanine and glycine-D-phenylalanine (L- and D-**78**). The binding constants were K(**77b**+L-**78**) $= 1.3 \times 10^4$ M^{-1} and K(**77b**+D-**78**) $= 1.9 \times 10^4$ M^{-1}. When the diastereomers **76b** and **77b** were interacted with $TbCl_3$, the energy transfer between the donor tryptophan units of **76b** and the acceptor Tb^{3+} was found to be almost twice as efficient as the energy transfer between **77b** and Tb^{3+}. This indicates a significant intramolecular chiral discrimination due to the difference in the distance between the coordinatively trapped Tb^{3+} and the tryptophan groups in these diastereomeric complexes. Without the crown ether, there was very little energy transfer between $TbCl_3$ and pyreneacetamide (PyNHAc).

Significant excimer emission was observed for **76c** and **77c** (2.0×10^{-6} M) because of the intramolecular interaction of the pyrene units. This intramolecular excimer was strongly influenced by solvents. In alcohols such as methanol and ethylene glycol the excimer emission predominated, and in CH_2Cl_2, THF, and DMF, both the monomeric pyrene emission and its excimer emission coexisted. No excimer emission was observed for PyNHAc (8.0×10^{-6} M) in THF. Addition of KCl to **76c** in THF enhanced the excimer emission at the expense of the monomer emission. Since KCl could not quench the fluorescence of PyNHAc, the observed excimer enhancement was attributed to a closer interaction between the pyrene units after K^+ bound to the crown ether ring of **76c**. The crown ethers **76c** and **77c** were found to quench the fluorescence of glycine-L-tryptophan (L-**79**) in THF differently. Because of energy transfer, this in turn enhanced the fluorescence of **76c** and **77c**. On the basis of the fluorescence measurement, the following binding constants were obtained: K(**77c**+L-**79**) $= 1.2 \times 10^5$ M^{-1} and K(**77c**+L-**79**) $= 5.0 \times 10^4$ M^{-1}, corresponding to a chiral recognition factor of 2.4. These binding constants were 2.5−10 times greater than those of L- or D-**78** with **77b** in methanol.

3.3. Using Cyclodextrins

Cyclic oligosaccharides containing six, seven, and eight D-glucopyranose units are named as α-, β-, and γ-cyclodextrins with internal diameters of 5.7, 7.8, and 9.5 Å, respectively. These compounds can bind various organic compounds inside their hydrophobic cavities in aqueous solutions. Chromophores have been linked to cyclodextrins to build spectroscopic sensors for organic molecules.[49−51]

The β-cyclodextrin-based sensor molecules **80** and **81** were prepared by Corradini and co-workers.[52] These compounds had a chiral binding site for Cu(II) derived from phenylalanine and a dansyl fluorophore. Compound **80** contained an (*R*)-phenylalanine unit, and **81** contained an (*S*)-phenylalanine unit. Complexation of **80** and **81** with Cu(II) quenched the fluorescence of the dansyl group. The fluorescence quenching of **81** was greater than that of **80**, indicating a stronger Cu(II) coordination of **81** than **80**.

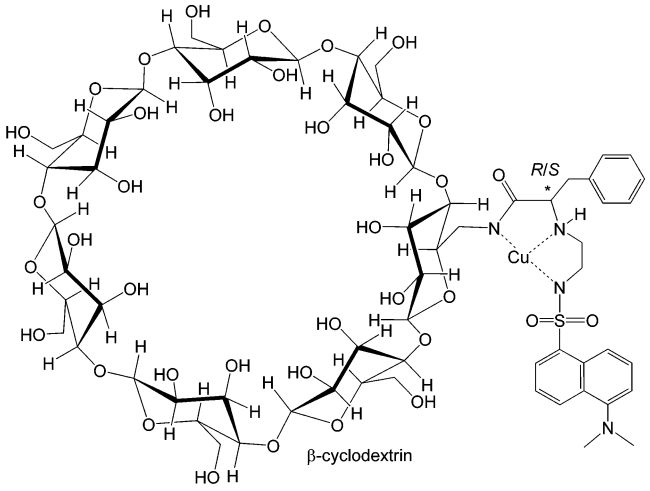

80+Cu^{2+} contains a (*R*)-phenylalanine unit
81+Cu^{2+} contains a (*S*)-phenylalanine unit

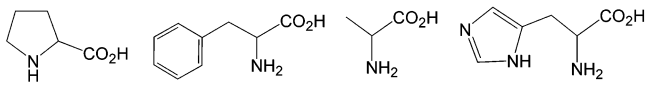

Proline **82** Phenylalanine **83** Alanine **84** Histidine **85**

Addition of amino acids was able to turn on the fluorescence since coordination of amino acids to Cu(II) displaced the sulfonamide of the dansyl group.

The authors studied the interaction of **80** + Cu(II) and **81** + Cu(II) with both enantiomers of the amino acids **74** and **82**−**85**. The best enantioselective fluorescence response was observed when **81** + Cu(II) (6×10^{-5} M aqueous solution pH = 7.3) was interacted with an equimolar amount of D- or L-proline (**82**), which gave $\Delta F_D/\Delta F_L = 3.89$ (ef). Complex **80** + Cu(II) had reversed and also much smaller enantioselectivities with the highest observed for its interaction with proline ($\Delta F_L/\Delta F_D = 0.74$). Histidine (**85**) caused the largest fluorescence enhancement for the fluorophores but with almost negligible enantioselectivity.

Yang and Bohne reported the interaction of β-cyclodextrin−pyrene complex with D- and L-tryptophan (**74**).[53] Pyrene was known to form 1:1 and 1:2 complexes with β-cyclodextrin in aqueous solution which gave rise to a new peak at a longer wavelength in the UV absorption spectrum. Addition of tryptophan to the pyrene−β-cyclodextrin complex led to efficient fluorescence quenching between 365 and 400 nm while excited at the isobestic point 337 nm. This fluorescence quenching was dramatically inhibited in the presence of alcohols or sulfates. Thus, a much higher concentration of tryptophan (5−25 mM) was needed to quench the fluorescence of pyrene and β-cyclodextrin with alcohols or sulfates. The authors found, that in the presence of *t*-BuOH (20 mM), the fluorescence quenching of the complex of pyrene (0.97 μM) with β-cyclodextrin (13 mM) by D- and L-tryptophan (5−25 mM) showed a large difference in the water/methanol solution. The ratio of K_{SV}(D-Trp)/K_{SV}(L-Trp) was up to 3.6 with K_{SV}(D-Trp) = 5 and K_{SV}(L-Trp) = 1.4 M^{-1}. D-Tryptophan quenched the fluorescence of pyrene more efficiently than L-tryptophan. Lower enantioselectivity was observed when

t-BuOH was replaced with *sec*-BuOH, *n*-BuOH, butyl sulfate, or hexyl sulfate. Without these additives, essentially no enantioselectivity was detected for the fluorescence quenching.

A static quenching mechanism was established as the same fluorescence lifetime was observed for pyrene with or without tryptophan in this system. One of the hypotheses to account for the observed chiral discrimination involved the formation of a complex between pyrene and tryptophan within the cavity of β-cyclodextrin. This close interaction and a charge transfer between pyrene and tryptophan upon excitation might have caused the observed significant enantioselective response in fluorescence quenching.

3.4. Using Macrocyclic Tubocurarine

The alkaloid (+)-tubocurarine (TC) existed in the zwitterionic form **86** at pH 9.[54] It gave an emission at 337 nm with $\lambda_{exc} = 280$ nm. Yatsimirsky and coworkers studied the interaction of **86** with amino acids in 0.03 M borate buffer solution of pH 9.0.

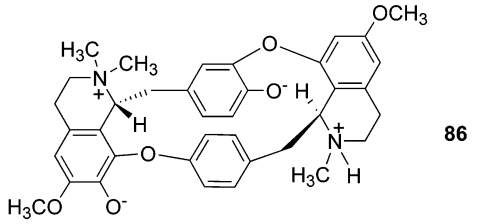

86

zwitterionic form of (+)-tubocurarine (TC) macrocycle

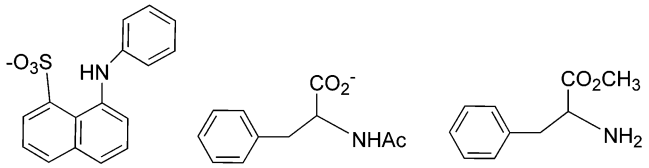

87 **88** **89**

Direct titration of **86** with amino acids gave scattered curves with an overall fluorescence intensity change within 10% of the original value. Compound **86** was then complexed with a fluorescence label, 8-anilinonaphthalenesulfonate anion (**87**). In the presence of **86** (20 mM), the fluorescence intensity of **87** (5.04 μM) was increased by almost 1 order of magnitude and its emission shifted to a shorter wavelength. A linear relationship was observed between the fluorescence intensity of **87** and the concentration of **86** measured at $\lambda_{emi}/\lambda_{exc} = 516/367$ nm. When a highly fluorescent **86** + **87** complex (5.04 μM/0.91 mM) was titrated with the enantiomers of the amino acids **88** and **89** (0−0.015 M), a dramatic enantioselective response was observed. Compounds D-**88** and D-**89** greatly increased the fluorescence intensity of **86** + **87**, but L-**88** and L-**89** significantly decreased the fluorescence intensity. The fluorescence enhancement represented the formation of ternary complexes, and the decrease in fluorescence indicated the displacement of the complexed **87**. The binding of amino acids with **86** was also studied by ^{1}H NMR and UV spectroscopic methods.

3.5. Using Proteins and Enzymes

The interaction of bovine α-acid glycoprotein (AGP) with D- and L-dansyl phenylalanine (**90**) in water solution was reported by Yan and Myrick.[55] Compounds D- and L-**90** displayed an emission maximum at 544 nm ($\lambda_{exc} = 200$ nm). Treatment of **90** with

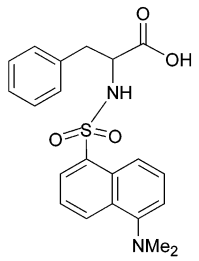

dansylphenylalanine
90

excess AGP significantly changed the fluorescence of the dansyl amino acid. A new emission peak was observed at 497 nm ($\lambda_{exc} = 220$ nm) where the intensity of D-**90** was much higher than that of L-**90**. This 47 nm hypsochromic shift might be the result of a change of the local environment of D-**90** and L-**90** from hydrophilic to hydrophobic after binding with AGP. Quenching of the fluorescence of AGP at 340 nm ($\lambda_{exc} = 220$, 280 nm) was also observed with a slightly greater effect by D-**90** than by L-**90**. When the concentration of AGP was set at 24 μg/mL, the fluorescence intensity of **90** at 497 nm showed a linear increase with the concentration of **90** (0−0.75 μM). In this plot, the slope ratio of D-**90** versus L-**90** was 2.64, indicating a significant chiral discrimination. AGP bound D-**90** better than L-**90**. In the fluorescence measurement, the authors also applied the principal component regression, a chemometric method, to determine the concentration of D-**90** and L-**90** in an enantiomeric mixture because the new emission maximum after bound to AGP overlapped with the original fluorescence spectra of **90**.

Bovine serum albumin (BSA) bound chiral stationary phases have been used in HPLC. The binding of BSA with the dansyl amino acids [1×10^{-6} M in 25 mM phosphate buffer (pH 7)/^{i}PrOH (95:5)] L-**91**, D-**91**, L-**92**, and D-**92** (1−20 equiv) was studied by Abe et al.[56] They measured the fluorescence intensity increase of the dansyl amino acids ($\lambda_{emi} = 488-508$ nm, $\lambda_{exc} = 335-351$ nm) when bound with BSA. These experiments showed that the association constants of BSA with the dansyl amino acids were 6.13×10^4 M^{-1} for L-**91**, 2.98×10^4 M^{-1} for D-**91**, 1.79×10^4 M^{-1} for L-**92**, and 4.57×10^4 M^{-1} for D-**92**. BSA was found to have multiple binding sites for the amino acids. Compounds L-**93** and D-**94** (1−3 equiv) were added to the mixture of BSA (2×10^{-5} M) and the dansyl amino acids (2×10^{-6} M) in the same solution as above. Because the naphsyl amino acids were not fluorescent, their displacement of BSA-bound dansyl amino acids led to fluorescent decrease. The order of the fluorescence decrease, corresponding to the degree of the displacement, was D-**91** > L-**92** > L-**91** > D-**92** when using L-**93**, and L-**92** > D-**92** ∼ D-**91** > L-**91**

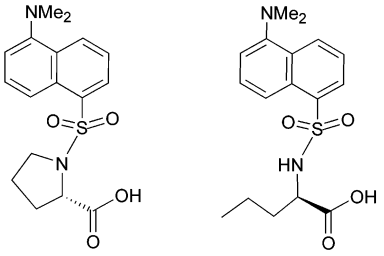

DNS-L-Proline
L-**91**

DNS-D-norvaline
D-**92**

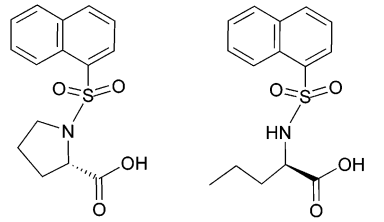

Naphsyl-L-Proline
L-**93**

Naphsyl-D-norvaline
D-**94**

when using D-**94**. According to the association constants, L-**91** bound BSA more strongly than D-**92**. It means that D-**92** should be displaced more easily than L-**91**, which was opposite to what was observed when L-**93** was used. This indicates that the binding sites of L-**91** and D-**92** on BSA were different. The different binding orders observed when using L-**93** and D-**94** for the competitive adsorption also demonstrated that they bound to different sites on BSA.

The competitive replacement of bovine serum albumin (BSA) bound L-**91** and D-**92** with carbazole carbonyl (CC)-amino acids was studied by monitoring the fluorescence at 488 nm for the emission of L-**91** (λ_{exc} = 343 nm) and at 508 nm for the emission of D-**92** (λ_{exc} = 335 nm).[57] The BSA bound L-**91** and D-**92**

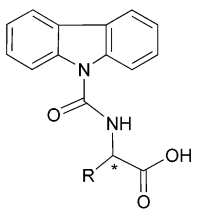

R = CH_3 (Ala), aminobutyric acid (ABA),
n-C_3H_7 (norVal), n-C_4H_9 (norLeu)

carbazole carbonyl amino acids (CC-amino acids)

exhibited much stronger fluorescence than the unbound ones by about 1 order of magnitude. Thus, replacement of the BSA-bound L-**91** or D-**92** led to significant decrease in fluorescence intensity. It was found that the displacement of L-**91** (10^{-6} M) on BSA (10^{-5} M) by CC-D-amino acids (10−30 equiv of L-**91**) was greater than that by CC-L-amino acids. For example, CC-L-Ala could not displace L-**91** at all while CC-D-Ala led up to 30% reduction in the fluorescence intensity. The displacement of the BSA bound D-**92** by CC-amino acids was much smaller with little chiral discrimination compared to the BSA bound L-**91**.

Kumar et al. found that addition of BSA to *N*-[4-(1-pyrene)butyroyl]-D-phenylalanine (D-**95**) caused a significant red shift with increased absorbance for the UV absorptions of D-**95**.[58] However, a decrease in

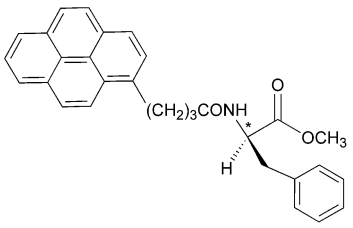

D-**95**

absorbance was observed when BSA was titrated into the solution of L-**95**. The UV measurement showed that L-**95** bound BSA 100 times more strongly than did D-**95** ($6.7 \times 10^7/5.3 \times 10^5$ M). The fluorescence spectra of the mixture of L-**95** or D-**95** (2 μM) with BSA (0−20 μM) were studied while excited at 344 nm (the isosbestic point). It was found that increasing the concentration of BSA increased the fluorescence intensity of D-**95**, which then reached a plateau of 2-fold enhancements. In contrast, the fluorescence of L-**95** was strongly quenched by BSA. When the amino ester−BSA complexes were treated with $Co(NH_3)_6Cl_3$, a fluorescent quencher, the fluorescence of L-**95** + BSA was further quenched but that of D-**95** + BSA was further enhanced. These dramatic differences in fluorescence responses demonstrated that the binding environments of the two enantiomeric amino esters on BSA were very different.

Gafni studied the fluorescence quenching of ϵNAD$^+$ (nicotinamide 1,N^6-ethenoadenine dinucleotide) bound to liver alcohol dehydrogenase (LADH) ($\lambda_{emi}/\lambda_{exc}$ = 400/312 nm) by D-, L-, and racemic methionine (**96**).[59]

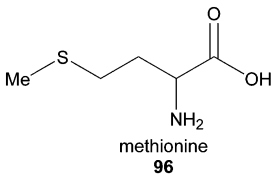

methionine
96

In 0.05 M phosphate buffer (pH 7.3), quenching of the fluorescent ethenoadenine ring in the ternary complex of 1.2×10^{-5} M of both LADH and ϵNAD$^+$ and 1.7 mM pyrazole by **96** gave linear Stern−Volmer plots. The quenching constants were k_q^L = 8.4×10^7 M^{-1} s^{-1}, k_q^D = 3.0×10^7 M^{-1} s^{-1}, and k_q^{DL} = 5.9×10^7 M^{-1} s^{-1}. The ratio of the quenching constants of the two enantiomeric D- and L-**96** was $k_q^L/k_q^D \approx 3$. The racemic **96** had the averaged quenching efficiency of the two enantiomers.

3.6. Using Copper(II) Complexes

In the reversed phase HPLC separation of racemic DNS-amino acids **97a**−**c** using the bis(L-phenylalanylamidato)copper(II) complex **98** as an additive and a fluorescence detector, Marchelli and co-workers found that the peak area of the D-amino acid **97** was always larger than that of its L-enantiomer.[60] They then studied the fluorescence and excitation spectra of D-/L-**97a** and D-/L-**97b** with/without the chiral copper(II) complex **98**. Compounds **97** had an emis-

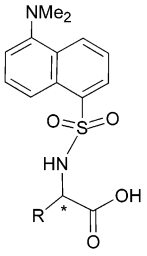

97

97a: DNS-Phenylalanine, R = $PhCH_2$
97b: DNS-Glutamic acid, R = $CH_2CH_2CO_2H$
97c: DNS-Aspartic acid, R = CH_2CO_2H

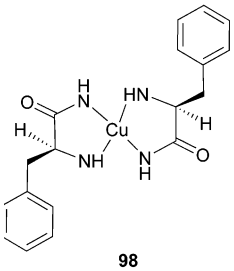

98

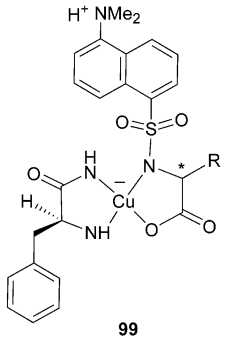

99

sion peak at 545 nm while excited at 330 nm in H_2O-CH_3CN (80:20). Addition of **98** (up to 6 equiv) significantly quenched the fluorescence of **97** (6×10^{-5} M in 80:20 H_2O-CH_3CN solution buffered at pH 7.5 with 0.3 M AcONa) but caused no change in the shapes and maxima of the emission and excitation spectra. The L-enantiomers of **97** were always quenched by the copper complex more than the D-enantiomers. The chiral discrimination for the enantiomers of **97b** [$K_{SV}(L)/K_{SV}(D) = 2.1$ ($10^{3.57}/10^{3.24}$)] was much larger than that for **97a** [$K_{SV}(L)/K_{SV}(D) = 1.3$ ($10^{3.55}/10^{3.44}$)] as demonstrated by their Stern–Volmer plots.

Complex **98** quenched the fluorescence of **97** much more efficiently than copper(II) alone. Study of the fluorescence lifetime of **97a** in the presence of **98** concluded that static quenching was the most likely mechanism since more than 90% of the observed fluorescence was due to a component of 8.9 ns lifetime independent of the concentration of copper(II) or **98**. The different stability of the different diastereomers of **99** generated from the reaction of **98** with **97** was proposed to account for the fluorescence quenching and enantioselectivity.

4. Enantioselective Fluorescent Recognition of α-Hydroxycarboxylic Acids by 1,1′-Binaphthyls

Chiral α-hydroxycarboxylic acids are very useful synthons for many organic natural products and drug molecules. Fluorescent sensors that can distinguish the enantiomers of an α-hydroxycarboxylic acid will be useful in the high throughput screening of chiral catalysts for the asymmetric synthesis of these chiral compounds. 1,1′-Binaphthyl-based acyclic and macrocyclic compounds were used by Pu and co-workers to carry out the enantioselective fluorescent recognition. Their fluorescence signals can be enhanced in the presence of α-hydroxycarboxylic acids because of the acid inhibited photoinduced electron transfer (PET).

4.1. Acyclic 1,1′-Binaphthyl Fluorophores[61,62]

Pu and co-workers designed the chiral bisbinaphthyl molecule **100** for the fluorescent recognition of α-hydroxycarboxylic acids. This compound contained two (*S*)-binaphthyl units. Structure **101** was a proposed complex between **100** and (*S*)-mandelic acid which featured three specific hydrogen bonds. A central nitrogen atom was incorporated into **100** to quench the fluorescence of the binaphthyl units by a PET process. When compound **100** was treated with an α-hydroxycarboxylic acid, the interaction of the nitrogen with the acid proton as indicated in the proposed complex **101** was expected to inhibit the PET process and enhance the fluorescence.

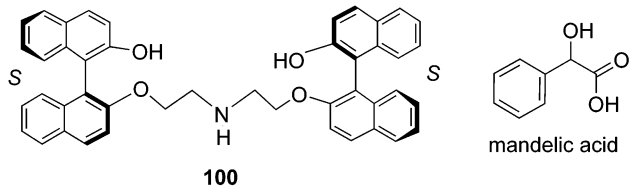

100

mandelic acid

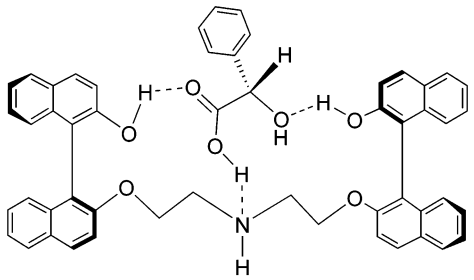

101

Compounds **102** and **103**, the dendritic derivatives of **100** with phenylene dendrons, were also synthesized. Compound **102** was the G0 dendrimer, and compound **103** was the G1 dendrimer. They both contained two (*R*)-binaphthyl units. These dendritic arms were introduced to improve the fluorescent properties of the core compound **100**.

In the UV spectra of these compounds, there were large increases in the absorptions at the short wavelengths (<300 nm) from the core to the G0 and G1 compounds because of the increasing number of branching phenyl rings at the 6,6′-positions of the binaphthyl units, but their long wavelength absorptions showed much smaller changes. The absorption maxima and extinction coefficients for these compounds were 280 (16500) and 334 (10600) nm for the core **100**, 263 (168700), 297 (sh, 53200), and 343 (sh, 9800) nm for **102**, and 267 (257100), 304 (sh, 58600), and 343 (sh, 9800) nm for **103**.

The dendritic branching benzene rings of the G0 and G1 compounds greatly increased their fluorescence intensity over that of the core **100**, indicating an efficient intramolecular energy transfer from the phenyl rings to the naphthyl core. The fluorescence maxima were observed at 372 nm for both **102** and

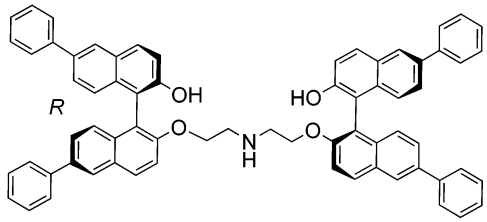

102

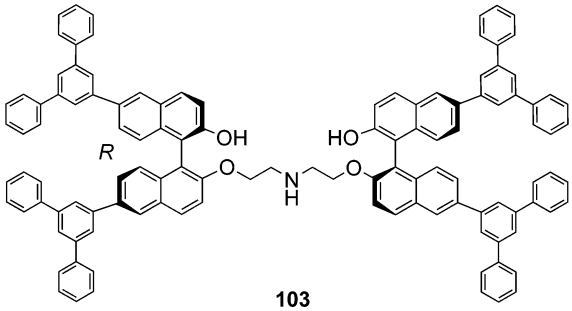

103

103 and 368 nm for **100**. In the excitation spectra, the most intense signals for **102** and **103** were observed at 270 nm where the phenyl rings absorb, consistent with an efficient intramolecular energy migration.

The fluorescence responses of these compounds toward mandelic acid were studied. In the presence of (*R*)- or (*S*)-mandelic acid, compound **100** exhibited a significant fluorescence enhancement because of a suppressed PET quenching when the acidic proton of mandelic acid interacted with the nitrogen of the bisbinaphthyl compound. This fluorescence enhancement was found to be very enantioselective. In benzene solution [containing 2% dimethoxyethylene (DME)], the fluorescence intensity of **100** (9.5×10^{-5} M) was increased to 2.87 times the original value by (*S*)-mandelic acid (5.0×10^{-3} M). However, (*R*)-mandelic acid (5.0×10^{-3} M) only increased the fluorescence intensity of **100** to 1.75 times the original value. That is, the enantiomeric fluorescence difference ratio, ef [ef = $(I_S - I_0)/(I_R - I_0)$], was 2.49. This large difference in the enantiomeric fluorescence enhancement made compound **100** practically useful for the enantioselective recognition of the chiral α-hydroxycarboxylic acid.

The fluorescence enhancement of the sensor followed the Benesi−Hildebrand type equation which gave the association constant of **100** + (*S*)-mandelic acid as 348 M^{-1}, and that of **100** + (*R*)-mandelic acid as 163 M^{-1}. The Job plot of the sensor in the presence of the acid indicated the formation of a 1:1 complex between the sensor and the acid. The fluorescence enhancements of the enantiomer of **100** in the presence of (*R*)- and (*S*)-mandelic acid had a mirror image relationship with those of **100**. This confirmed that the observed different fluorescence enhancement between the two enantiomers of mandelic acid was indeed due to chiral recognition by the fluorescent sensor. When **100** was treated with mandelic acid of various enantiomeric compositions, a linear relationship between I/I_0 and the percent of the *S* component of mandelic acid was observed. Thus, the enantiomeric composition of the α-hydroxycarboxylic acid could be readily determined by measuring the fluorescence intensity of sensor **100** in the presence of the substrate.

The derivatives of mandelic acid, compounds **104** and **105**, were also used to interact with the chiral fluorophore **100**. The α-hydroxyl group in **104** was protected with an acetyl group, and the acid group of **105** was converted to a methyl ester. Both of the

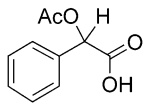

104

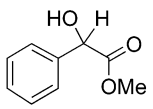

105

enantiomers of **104** were found to greatly enhance the fluorescence of **100** but exhibited almost no enantioselectivity. Compound **105** could not enhance the fluorescence of **100** under the same conditions as the use of mandelic acid. These observations demonstrated that both the hydroxyl group and the carboxylic acid group of mandelic acid were important for the enantioselective fluorescent recognition by the chiral binaphthyl receptor. It supported the proposed multiple hydrogen bonding interaction between **100** and mandelic acid as shown by **101**.

The fluorescence responses of the G0 and G1 dendritic derivatives **102** and **103** toward mandelic acid were studied. As the dendritic generation increased, the fluorescence enhancement of the chiral bisbinaphthyl compounds in the presence of the acid also increased significantly. The fluorescence enhancement ($I - I_0$) of **102** by (*R*)-mandelic acid was 14 times that of (*R*,*R*)-**100**, and the fluorescence enhancement of **103** by (*R*)-mandelic acid was 22 times that of (*R*,*R*)-**100**. Therefore, the dendritic branches of the G0 and G1 compounds not only generated more intense fluorescence signals than the core but also greatly amplified the fluorescence responses of the core toward the α-hydroxycarboxylic acid. That is, the G0 and G1 molecules were much more sensitive fluorescent sensors than the core. The enantioselectivity of the G0 molecule **102** was similar to that of the core with an ef value of 2.05. The enantioselectivity of the G1 molecule **103** was a bit lower with an ef of 1.49. The G0 dendrimer **102** was therefore considered as the best choice among these chiral fluorophores because of its high sensitivity as well as good enantioselectivity.

4.2. Macrocylic 1,1′-Binaphthyl Fluorophores[45,46]

Pu and co-workers found that the bisbinaphthyl macrocycles (+)- and (−)-**63** were not only useful in the enantioselective fluorescent recognition of amino acid derivatives (see discussions in 3.1) but also useful for the recognition of α-hydroxycarboxylic acids.[45] Treatment of (−)-**63** with (*S*)-mandelic acid led to greatly enhanced fluorescence especially at λ_{long} (424 nm). However, very little fluorescence enhancement at λ_{long} was observed when (−)-**63** was interacted with (*R*)-mandelic acid under the same conditions. Thus, (−)-**63** had exhibited an extremely high

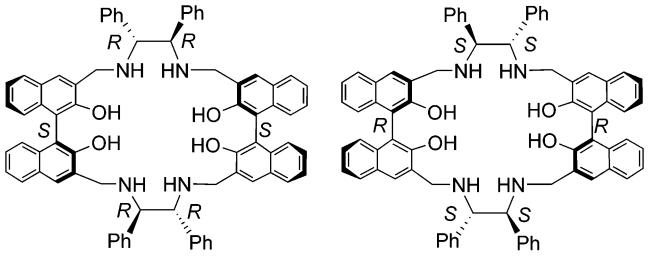

(-)-**63** (+)-**63**

enantioselective fluorescent response toward the chiral acid. In a concentration range of 5.0×10^{-3} to 2.0×10^{-2} M of (*R*)- and (*S*)-mandelic acid in benzene containing 2% DME, the fluorescence enhancement of (−)-**63** (1.0×10^{-4} M) at λ_{long} was studied (λ_{exc} = 340 nm). An ef $[(I_S - I_0)/(I_R - I_0)]$ of over 12 was observed. The chiral recognition was confirmed by using the enantiomeric macrocycle (+)-**63** to interact with (*R*)- and (*S*)-mandelic acid.

The Job plot for the interaction of (+)-**63** with (*R*)-mandelic acid, obtained by ^{1}H NMR measurements, indicated the formation of a 1:4 complex among other possible binding forms between the macrocycle and the acid. It was expected that these complexes involved the binding of the nitrogen atoms of the macrocycle and the acidic proton of the acid. This interaction inhibited the PET fluorescence quenching of the macrocycle by its nitrogen atoms, leading to the enhanced fluorescence. The fluorescence measurements suggested that (*R*)-mandelic acid should bind (+)-**63** more strongly than (*S*)-mandelic acid and (*S*)-mandelic acid should bind (−)-**63** more strongly than (*R*)-mandelic acid. The relationship between the fluorescence intensity of (−)-**63** at λ_{long} and the enantiomeric composition of mandelic acid was found to be close to linear. Thus, the chiral bisbinaphthyl macrocycle could be used as a fluorescent sensor to readily determine the enantiomeric composition of mandelic acid.

Macrocycle (−)-**63** was also used to interact with hexahydromandelic acid. In the concentration range of 5.0×10^{-3} M to 2.0×10^{-2} M, (*S*)-hexahydromandelic acid enhanced the fluorescence of (−)-**63** at λ_{long} significantly, but (*R*)-hexahydromandelic acid did not.

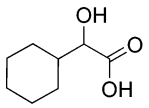

hexahydromandelic acid

The fluorescence enhancement of (−)-**63** by (*S*)-hexahydromandelic acid was smaller than that by (*S*)-mandelic acid. A linear relationship between the fluorescence intensity of (−)-**63** and the enantiomeric composition of hexahydromandelic acid was also obtained.

The 6,6′-substituted compounds **71** and **72** were used for the fluorescent recognition of mandelic acid in methylene chloride solution.[46b] Large fluorescence enhancement of the 6,6′-*p*-ethoxyphenyl substituted macrocycle **71** at λ_{short} was observed when treated with mandelic acid. In the meantime, the long wavelength emission was either quenched or unchanged. The fluorescence enhancement at λ_{short} was enantioselective with an ef ca. 2. This fluorescence enhancement at λ_{short} of **71** was similar to that of the unsubstituted macrocycle **63** in methylene chloride except that the fluorescence intensity of **71** was much stronger and its fluorescence measurements could be conducted at concentrations of 2 orders of magnitude lower. The 6,6′-styryl substituted macrocycle **72** behaved similarly to **71** when treated with the enantiomers of mandelic acid. Both (*R*)- and (*S*)-mandelic acid quenched at λ_{long} of the macrocycle and enhanced at λ_{short}. The fluorescence enhancement at the short wavelength was enantioselective with an ef ca. 2.

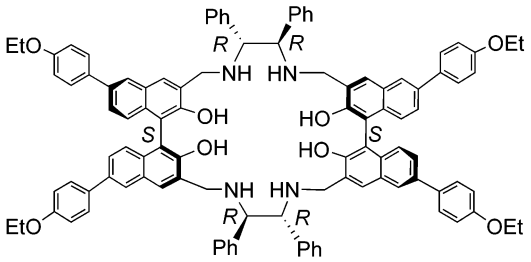

71

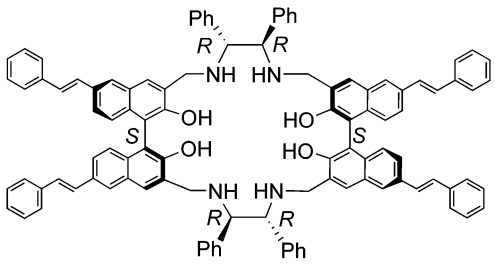

72

5. Enantioselective Fluorescent Recognition of Sugars by 1,1′-Binaphthyls

Fluorescent sensors have been developed for the recognition of sugars.[63] In this chapter, only chiral compounds that have shown enantioselective fluorescence responses to the enantiomers of sugars are discussed.

The (*R*)- and (*S*)-1,1′-binaphthyl diboronic acids (*R*)- and (*S*)-**106** were designed and synthesized for the fluorescent recognition of D- and L-monosaccharides by Shinkai and co-workers.[64] In 33.3% methanol and H_2O buffer at pH 7.77, **106** (1.0×10^{-5} M) displayed an emission maximum at 358 nm with excitation at 289 nm. Addition of monosaccharides enhanced the fluorescence intensity of **106**. For example, D-glucose enhanced the fluorescence of **106** up to 4 times the original intensity. Saccharides could form cyclic boronate esters with the boronic acid groups of **106**. This increased the Lewis acidity of the boronic acids, leading to their stronger interaction with the adjacent tertiary amine. The PET fluorescence quenching of the naphthyl fluorophores by the nitrogen atoms could therefore be inhibited and give the enhanced fluorescence. Formation of a 1:1 complex between **106** and a monosaccharide with two cyclic boronate esters, such as **107**, was proposed.

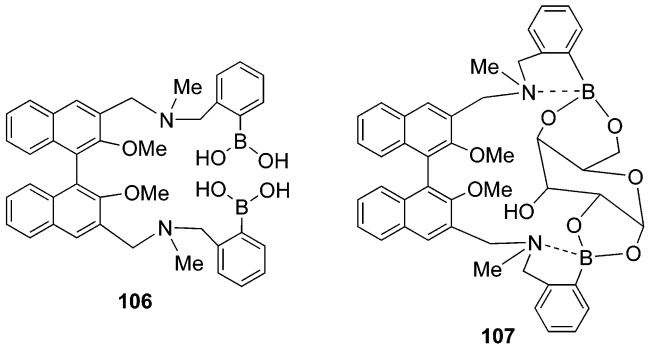

106 107

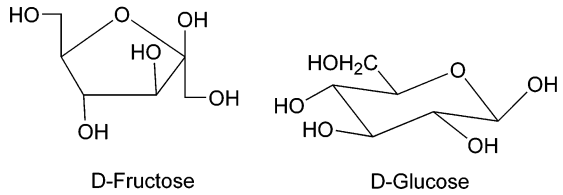

D-Fructose D-Glucose

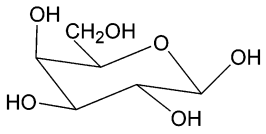

D-Galactose

The fluorescence enhancement of **106** by monosaccharides was found to be enantioselective. The fluorescence intensity ratio for the interaction of (*R*)-**106** with D-/L-fructose was 1.47, with D-/L-glucose 1.93, and with D-/L-galactose 0.82. The chiral recognition was attributed to the stability difference between the diastereomeric complexes formed from the reaction of (*R*)- or (*S*)-**106** with the D- and L-sugars. The ratio of the association constants for the interaction of (*R*)-**106** with D- and L-sugars was 3.2 for D-/L-fructose, 1.6 for D-/L-glucose, and 0.62 for D-/L-galactose.

Another chiral binaphthyl diboronic acid, **108**, was also used for sugar recognition.[65] UV titration with NaOH showed that binding of **108** with D-glucose increased the acidity of the boronic acids and changed the pK_a from 10.7 to 10.2. The binding of monosaccharides with **108** caused little change in the UV absorption of **108**. However, fluorescence enhancement of (*R*)-**108** (1.00×10^{-5} M, water/MeOH = 100:1, pH 10.8 buffer) at 406 nm (λ_{exc} = 260 nm) was observed in the presence of D- or L-glucose (5.00×10^{-3} M). L-Glucose increased the fluorescence intensity of **108** up to 1.4 times the original value and D-glucose up to 1.2 times. The Job plot on the basis of CD measurements indicated the formation of a 1:1 complex such as **109**. The fluorescence enhancement was attributed to the much more rigid structure of **109**. Binding of (*R*)-**108** with L-glucose caused the emission maximum blue-shifted to 397 nm and with D-glucose red-shifted to 412 nm. Fluorescence enhancement in the range of a 1.07−1.30-fold increase was also observed when **108** was interacted with other monosaccharides such as fructose, talose, galactose, allose, mannose, and xylose. Although the differences in the fluorescence signals of **108** in the presence of D- and L-sugars were small, D- and L-xylose showed a large difference in association constants with D/L = 1.0/8.7. The complex of **108** with D-xylose was very unstable.

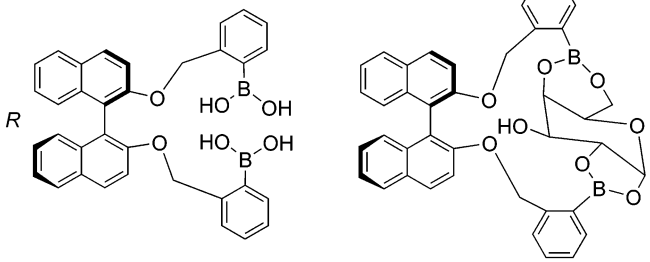

108 109

Addition of methyl α-D-glucopyranoside (**110**) generated no change for the fluorescence and CD spectra of **108**. This was attributed to the loss of the primary binding site of D-glucose after methylation. D-Glucose also could not enhance the fluorescence of the monoboronic acid **111**. These experiments further supported the hypothesis that the observed fluorescence enhancement of **108** in the presence of the monosaccharides was due to the formation of the rigid cyclic complex **109**.

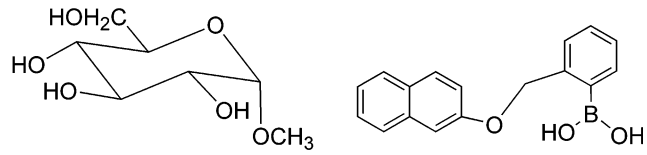

methyl α-D-glucopyranoside 111
110

6. Enantioselective Fluorescent Recognition of Other Chiral Organic Compounds Including Alcohols, Ketones, and Alkenes

It is much more difficult to carry out the enantioselective fluorescent recognition of compounds that do not possess functional groups such as amines and carboxylic acids because these substrates have much weaker interactions with the molecular receptors. Therefore, the recognition of simple chiral alcohols, ketones, and alkenes is remarkably underdeveloped. Among the reported work, the use of cyclodextrins is particularly noticeable. One of the recognition principles involving the competitive displacement of a fluorophore included inside the cyclodextrin cavity by simple chiral compounds may be of general use.

6.1. Using Cyclodextrins

Cyclodextrins were used to interact with both free and covalently bound *p*-(dimethylamino)benzoyl compounds.[66] Hamasaki et al. found that α-cyclodextrin did not bind ethyl 4-dimethylaminobenzoate **112** well due to its small cavity and the large cavity of γ-cyclodextrin could bind two molecules of **112** to form a 2:2 complex. Only the cavity size of β-cyclodextrin matched the size of **112**. When **112** was treated with β-cyclodextrin in an aqueous solution (10% acetonitrile), inclusion of **112** inside β-cyclodextrin led to significantly increased twisted intramolecular charger transfer (TICT) emission of **112** at

ca. 540 nm. The normal planar emission of **112** at 370 nm was greatly increased in the presence of either β- or γ-cyclodextrin. Compound **112** alone in solution did not show the TICT emission. The large cavity size of γ-cyclodextrin also did not cause much TICT emission for **112**. β- and γ-cyclodextrins induced much greater CD effects in **112** than α-cyclodextrin.

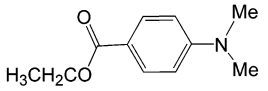

112

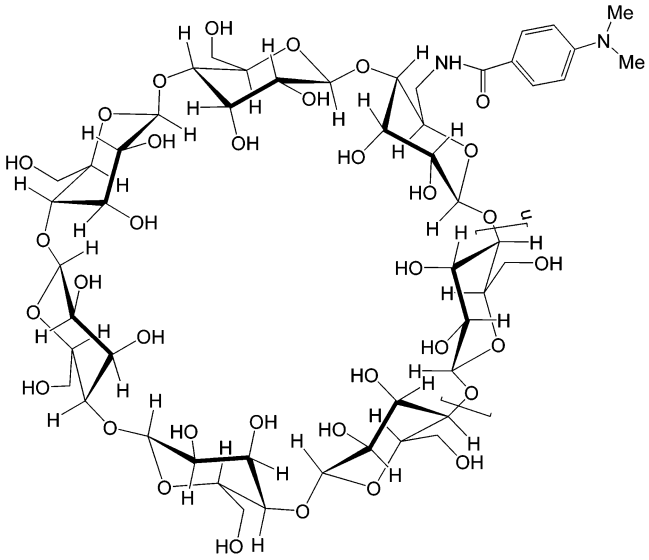

113: n = 0, α–cyclodextrin
114: n = 1, β–cyclodextrin
115: n = 2, γ–cyclodextrin

Modified α-, β-, and γ-cyclodextrins with a covalently bonded *p*-(dimethylamino)benzoyl, **113**−**115**, were prepared. Compound **114** gave a predominantly TICT emission at 495 nm in aqueous solution, but compounds **113** and **115** showed much weaker TICT bands. This observation together with the NMR and CD studies demonstrated that the *p*-(dimethylamino)benzoyl of **114** was tightly included inside the cyclodextrin cavity. The cavity of **113** was too small to include the *p*-(dimethylamino)benzoyl, and the cavity of **115** was too big to keep this group inside. The TICT emission of **114** was used to sense a number of guest molecules. When guest molecules such as 1-adamantanol were added to the solution of **114**, a large decrease of the TICT emission was observed, indicating the displacement of the *p*-(dimethylamino)benzoyl group by the guest molecule inside the cyclodextrin cavity. This fluorescence response of **114** was also found to be enantioselective when it was treated with *d*- and *l*-menthol (**29**). It gave $\Delta I/I° = 0.25$ for *d*-menthol and 0.36 for *l*-menthol ($\Delta I = I° - I$, and $I°$ and I are the TICT emission intensities in the absence and presence of a guest), i.e., an ef of 1.44.

Ueno et al. prepared the pyrene substituted γ-cyclodextrin compounds **116a** and **116b**.[67] The absorption and fluorescence spectra of these compounds exhibited significant concentration dependence. Cyclodextrins **116a** and **116b** were observed to form dimers with association constants of 1.74×10^5 and 1.53×10^4 M^{-1}, respectively. In a 10% DMSO aqueous solution, **116a** and **116b** exhibited an excimer emission around 470 nm together with the monomer emissions at 378 and 396 nm. The emission intensity ratios (I_{470}/I_{378}) of **116a** and **116b** were 4.2 and 1.1, respectively. The model compound **117** only showed the monomer emission with no excimer emission. Addition of a variety of organic molecules to **116a** and **116b** led to reduction of the excimer emission. Formation of the dimers **118** from **116a**,**b** in which the two included pyrenes could interact with each other inside the cyclodextrin cavity might account for the observed excimer emission (Scheme 3).

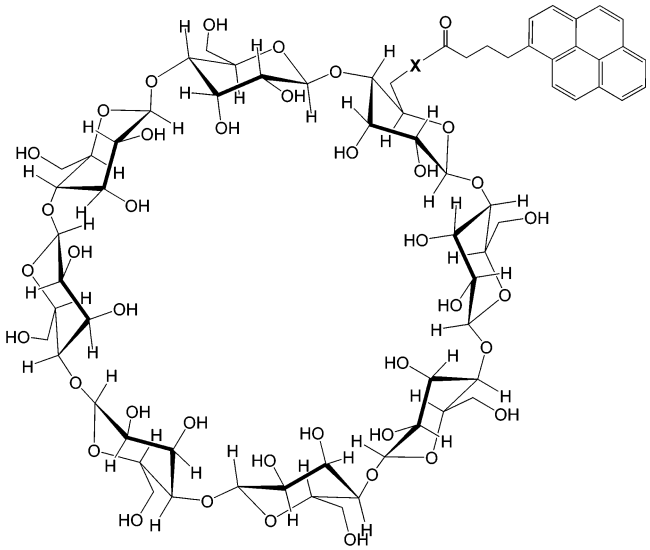

γ–cyclodextrin

116a: X = NH
116b: X = O

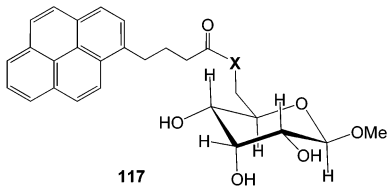

117

Scheme 3. Interaction of the Dimer 118 with a Guest Molecule

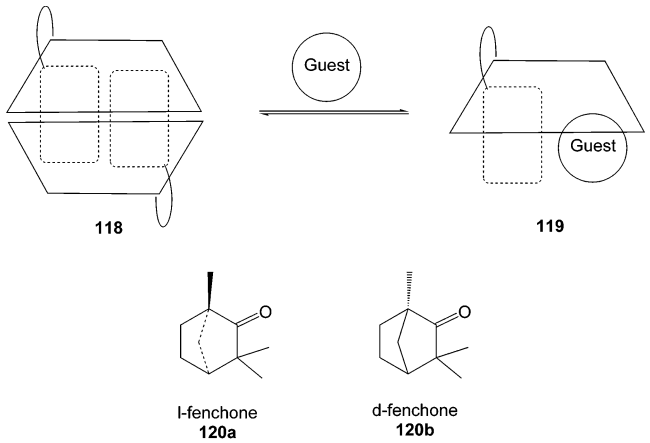

Table 2. The Fluoresence Responses of 116a,b in the Presence of 120a,b

	120a		120b	
fluorophore	$\Delta I_m/I_m^0$	$\Delta I_{ex}/I_{ex}^0$	$\Delta I_m/I_m^0$	$\Delta I_{ex}/I_{ex}^0$
116a	0.834	0.273	0.838	0.290
116b	0.180	0.342	0.149	0.353

Addition of a guest molecule could convert the dimer **118** to **119** to give reduced excimer emission. One pair of the enantiomers of fenchone (**120a**,**b**) were among the guest molecules studied. The change in the monomer emission of **116a**,**b** was measured at 378 nm and represented by $\Delta I_m/I_m^0$ ($\Delta I_m = I_m - I_m^0$). The change in the excimer emission was represented by $\Delta I_{ex}/I^0$ ($\Delta I_{ex} = I_{ex}^0 - I_{ex}$). In 10% DMSO aqueous solution, small chiral effects were observed when the fluorescence spectra of **116a**,**b** (3.0×10^{-5} M) were measured in the presence of **120a**,**b** (2 mM). As shown in Table 2, the enantioselective fluorescent effects were less than 20% between the two enantiomers of fenchone.

γ-Cyclodextrin derivatives **121**−**124** that contained two naphthyl groups at different positions of the ring were synthesized.[68] The CD spectrum of **122** (10% ethylene glycol aqueous solution) gave an exciton coupling band with a peak at 220 nm and a trough at 232 nm, indicating a counterclockwise twisting between the two naphthalene rings (*S* helicity) induced by the chiral γ-cyclodextrin ring. The CD spectra of **123** and **124** were similar to those of **122**, but that of **121** displayed some inverted CD signals. The fluorescence spectra of these compounds in 10% ethylene glycol aqueous solution gave almost pure monomer emission at ca. 375 nm. This indicated that it was difficult for the two naphthalene rings in these compounds to form a face-to-face complex. Addition of l-borneol (**125**, 2.0 mM) to these compounds (0.02 mM) led to fluorescence enhancement by 29−52%. This fluorescence enhancement may be because the added organic substrate could further reduce the interaction of the naphthyl rings with water. A number of other organic substrates, including cholic acid, deoxycholic acid, chenodeoxycholic acid, ursodeoxycholic acid, cyclohexanol, 1-adamantanecarboxylic acid, cyclododecanol, nerol, and geraniol, were also observed to increase the fluorescence intensity of compounds **121**−**124**. The two enantiomers of menthol enhanced the fluorescence of **121**−**124** by 5−19%, but almost no enantioselectivity was observed.

A β-cyclodextrin containing a covalently bound dansyl moiety, **126**, was reported by Corradini et al.[69] The crystal structure of **126** demonstrated that the dansyl group was included in the cyclodextrin cavity with the dimethylamino and sulfonyl groups on the opposite sides. This solid state structure was found to be consistent with the aqueous solution data obtained by ^{1}H NMR ROESY and CD spectral analyses. The fluorescence quantum yield of the dansyl group in **126** was significantly increased due to its inclusion in the cyclodextrin cavity. When **126** was interacted with (*R*)/(*S*)-camphor (**59**) and (*R*)/(*S*)-fenchone (**120a**,**b**) in a buffered aqueous solution with or without the addition of $CuCl_2$, fluorescence quenching was observed but with no enantioselective response. A model involving the in and out movement

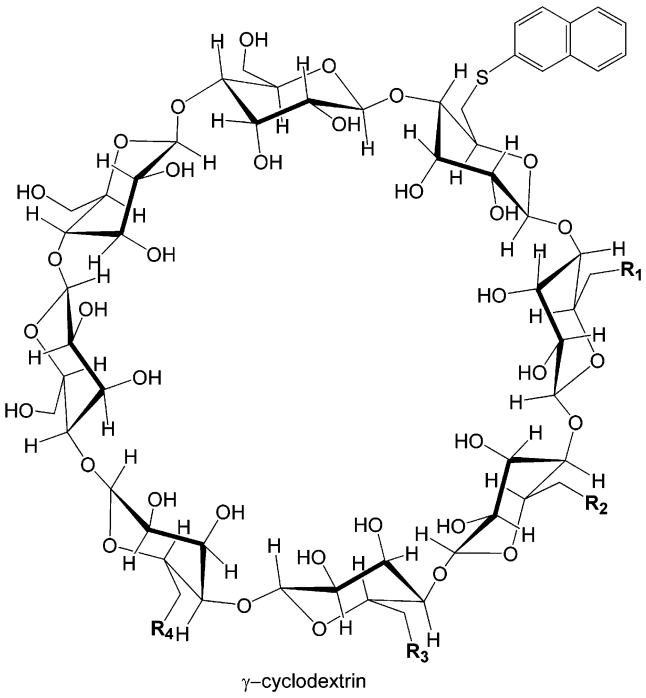

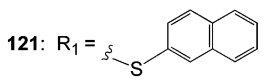

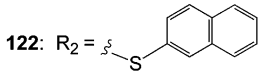

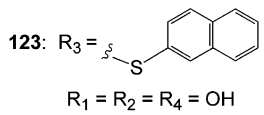

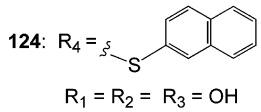

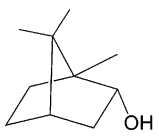

l-borneol
125

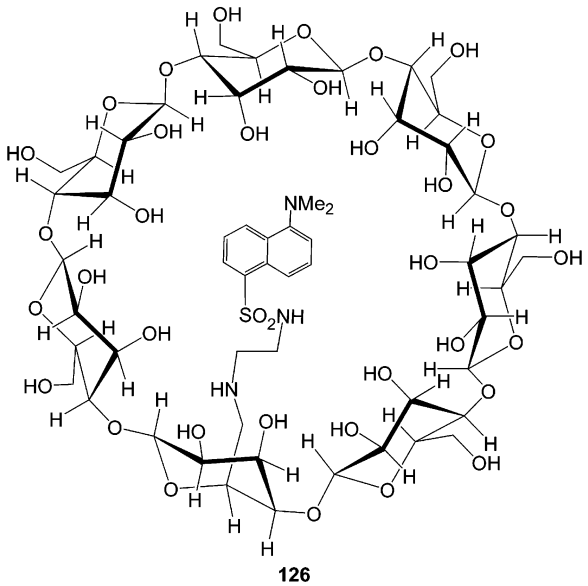

126

of the dansyl group from the cyclodextrin cavity was used to explain the fluorescence quenching.

6.2. Naphthyl Fluorophores

The laser induced fluorescence excitation spectra of racemic, (*R*)-, and (*S*)-2-naphthyl-1-ethanol (**127**) formed in a continuous supersonic expansion of helium was studied.[70,71] Zehnacker and co-workers found that all these compounds gave identical bands.

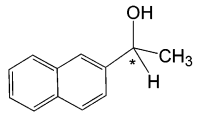

2-naphthyl-1-ethanol

127

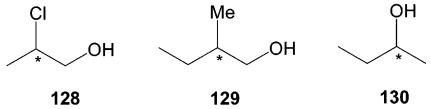

128 **129** **130**

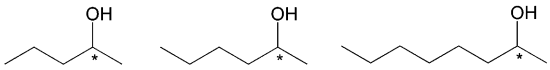

131 **132** **133**

Although complexing with achiral solvents such as methanol and 1-propanol showed no difference between (*R*)-**127** and (*S*)-**127**, the fluorescence excitation spectrum of (*R*)-**127** with (*S*)-2-chloro-1-propanol (**128**) displayed different peaks from (*S*)-**127** with (*S*)-**128**. The S_0-S_1 0−0 transition shifts ($\Delta\nu$) for (*S*)-NPOH + (*S*)-2-chloro-1-propanol were at −60 and −32 cm^{-1} and for (*R*)-**127** + (*S*)-**128** were −23 and +10 cm^{-1}. The interaction of **127** with other chiral alcohols including 2-methyl-1-butanol (**129**), 2-butanol (**130**), 2-pentanol (**131**), 2-hexanol (**132**), and 2-octanol (**133**) also showed chiral discriminations.

The interaction of **127** with a series of chiral terpenes in the supersonic jet was investigated.[72] The fluorescence excitation spectrum of the jet-cooled diastereoisomeric pairs formed by (*R*)-**127** + (*R*)-/(*S*)-α-pinene (**134**) showed very large differences. The

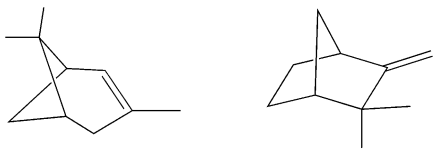

134 **135**

S_0-S_1 0−0 transition shift of (*R*)-**127** in the presence of (*R*)-**134** was −79 cm^{-1} ($\Delta\nu$) and in the presence of (*S*)-**134** −54 cm^{-1}. The fluorescence decay time was 34 ns for (*R*)-**127** + (*R*)-**134** and 44 ns for (*R*)-**127** + (*S*)-**134**. No difference was observed for the diastereomeric pair of (*R*)-**127** + (*R*)-/(*S*)-camphene (**135**) in the S_0-S_1 0−0 transition shift ($\Delta\nu = -35$ cm^{-1}), but their fluorescence decay time was different with 110 ns for (*R*)-**127** + (*R*)-**135** and 193 ns for (*R*)-**127** + (*S*)-**135**.

The interaction of (*R*)-**127** with (*R*)-/(*S*)-borneol (**125**) and camphor (**59**) that were capable of hydrogen bonding was also studied in the supersonic jet. The S_0-S_1 0−0 transition shift of (*R*)-**127** in the presence of (*R*)-borneol was −162 cm^{-1} and in the presence of (*S*)-borneol −191 cm^{-1}. No difference was observed for the diastereomeric pair of (*R*)-**127** + (*R*)-/(*S*)-camphor in the S_0-S_1 0−0 transition shift ($\Delta\nu = -89$ cm^{-1}), but their fluorescence decay time was different with 25 ns for (*R*)-**127** + (*R*)-camphor and 42 ns for (*R*)-**127** + (*S*)-camphor.

The fluorescence quenching of **127** in *n*-hexane solutions by (*R*)-/(*S*)-camphor was studied. When excited at 317 nm, the fluorescence quenching of **127** (3.1×10^{-3} M) was accompanied by enhancing the weak emission of camphor (1.12×10^{-2} M) in the visible region. This indicated that a singlet−singlet energy transfer from the naphthalene to the camphor was involved in the fluorescence quenching mechanism. In the (*R*)- and (*S*)-camphor concentration range of 10^{-3} to 2×10^{-2} M, linear Stern−Volmer plots were obtained which demonstrated enantioselective fluorescence quenching of (*R*)-**127**. It was found that $K_{SV}(R\text{-}R) = 51$ M^{-1} and $K_{SV}(R\text{-}S) = 39$ M^{-1}, i.e., $K_{SV}(R\text{-}R)/K_{SV}(R\text{-}S) = 1.23$. The fluorescence lifetime measurement of (*R*)-**127** gave $\tau_0 = 6.9$ ns, which showed a linear decrease with increasing (*R*)- and (*S*)-camphor concentrations. The concentrations of (*R*)- and (*S*)-camphor also affected the fluorescence lifetime of (*R*)-**127** differently.

The steady state fluorescence quenching of (*R*)-**127** by the diketones, (*R*)-/(*S*)-camphorquinone (**136**) and biacetyl (**137**), was also studied which gave the Stern−Volmer constants as 187, 193, and 190, respectively. Almost no chiral discrimination was observed in the case of (*R*)-/(*S*)-**136**. The fluorescence quenching of (*R*)-**127** was also found to enhance the fluorescence of the diketones due to the electronic energy transfer.

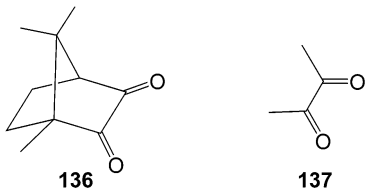

136 **137**

6.3. Using Proteins

Racemic- and (+)-gossypol (**138**) were isolated natural products that were potential drug candidates. Sampath and Balaram studied the binding of gossypol with human and bovine serum albumins.[73]

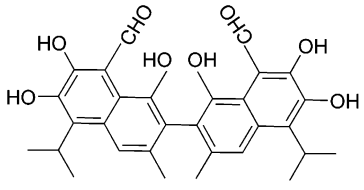

138

Quenching of the intrinsic fluorescence of the proteins at $\lambda_{emi} = 346$ nm ($\lambda_{exc} = 284$ nm) in phosphate buffer (pH 7.4) by racemic-, (+)-, and (−)-**138** was monitored. A single high affinity binding site on the proteins was detected. The K_D values with bovine serum albumins were $5.43 \pm 3.49 \times 10^{-8}$ M for (+)-

138, 7.98 ± 2.45 × 10^{-8} M for (−)-**138**, and 7.55 ± 1.84 × 10^{-8} M for (±)-**138**. The K_D values with human serum albumins were 6.63 ± 2.07 × 10^{-8} M for (+)-**138**, 7.38 ± 2.44 × 10^{-8} M for (−)-**138**, and 4.78 ± 0.42 × 10^{-8} M for (±)-**138**. Thus, the binding affinity of the enantiomers of **138** with the proteins was quite close.

7. Chiral Recognition in Excimer and Intramolecular Exciplex Formation

Excimers are complexes formed between an excited fluorophore and its ground state. When the fluorophore is chiral and racemic, the dimeric excimer will be composed of three isomers: one pair of enantiomers and a meso isomer. The enantiomeric pair and the meso isomer are diastereomers. A number of chiral molecules show chiral discrimination in the formation and dissociation of their excimers. The most extensively studied are pyrenes substituted with chiral amino acid units. Both intra- and intermolecular excimer formation were investigated. In general, the excimer emission gives a broad and structureless signal to the red of the local emission. The chirality of the fluorophores makes the diastereomeric excimers different in a variety of ways such as formation and dissociation rates, emission quantum yields and wavelengths, and lifetimes. Intramolecular exciplex formation of chiral molecules containing two different fluorophores is also discussed in this chapter.

7.1. Pyrene Derivatives

7.1.1. Intermolecular Excimer Formation

Tran and Fendler reported the excimer formation of *N*-[4-(1-pyrene)butanoyl]tryptophan (D- and L-**139**).[74] Emission of the pyrenyl amino acid derivatives, D-**139**, L-**139**, racemic **139**, and achiral **140** at 470 nm (a broad structureless band, red to the inherent emission of pyrene) increased with increasing concentration in methanol (1.0 × 10^{-3} to 1.0 × 10^{-2} M).

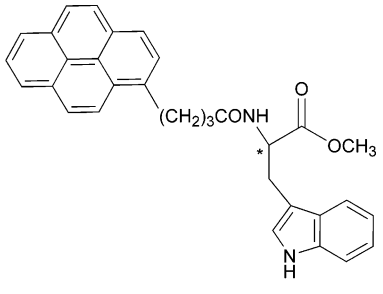

N-[4-(1-pyrene)butanoyl]-tryptophan

139

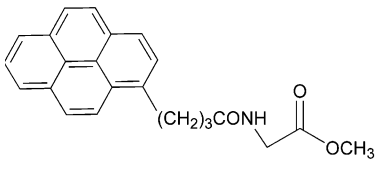

140

Because the behavior of **140** was similar to that of **139**, this emission was attributed to the formation of an excimer between two pyrene groups rather than the intra- or intermolecular pyrene−indole pairs. That is, the pyrene ring of one ground state molecule associated with the pyrene ring of an excited molecule to generate the excimer emission. Steady state and nanosecond time-resolved spectroscopy were conducted to determine the parameters for the excimer formation. It was found that the excimer formation rate constant was 6.9 × 10^9 M^{-1} s^{-1} for the racemic **139**, and 4.0 × 10^9 M^{-1} s^{-1} for the pure enantiomers. The free energy of the excimer formation was −2.6 kcal/mol for the pure enantiomer D- or L-**139**, and −3.3 kcal/mol for the racemic **139**. That is, there was a chiral discrimination energy of 0.7 kcal/mol. The kinetic and thermodynamic parameters of these pyrenyl compounds in (*R*)-, (*S*)-, and racemic 2-octanol (**133**) were also determined. The enthalpy of activation for the D-**139** excimer formation in (*R*)- and (*S*)−(+)-2-octanol gave a difference of 0.6 kcal/mol.

The excimer emission of (+)- or (−)-1-(1-hydroxyhexyl)pyrene, (+)- or (−)-**141**, in methanol at 460 nm was measured by Brittain et al.[75] This emission was

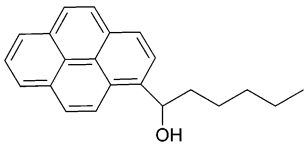

141

found to be partially circularly polarized. The circularly polarized luminescence (CPL) experiment allowed the measurement of both the total luminescence intensity (I) and the circularly polarized luminescence (ΔI) which gave the luminescence dissymmetry factor g_{lum} according to the following equation:

$$g_{lum} = \frac{2\Delta I}{I} = \frac{I_L - I_R}{\frac{1}{2}(I_L + I_R)}$$

In the equation, I_L and I_R are the intensity of left- and right-circularly polarized emitting light. Large dependence of g_{lum} on the concentration of (+)- or (−)-**141** was observed. No CPL was observed below 10^{-4} M. This indicated that the singlet excited state of (+)- or (−)-**141** contributed little to the g_{lum} ($<10^{-5}$). In the concentration range of 1 × 10^{-3} to 4 × 10^{-3} M (+)-**141**, g_{lum} increased from 1 × 10^{-3} to over 4 × 10^{-3}. The large CPL effects demonstrated that the excimer of (+)- or (−)-**141** should have a preferred chiral orientation of the pyrene rings.

De Schryver and co-workers reported the chiral discrimination of the intermolecular excimer of *N*-acetyl-1-pyrenylalanine methyl ester (**60**).[76] The fluorescence spectra of racemic **60** and its resolved enantiomers D- and L-**60** in the solutions of acetonitrile, toluene, and DMF were studied. In acetonitrile, the absorption spectrum of **60** showed no change with respect to the concentration increases. The excitation spectra of **60** at high concentration (10^{-2} M) analyzed at 378 (locally excited state) and 490 nm (excimer emission region) were similar. These observations

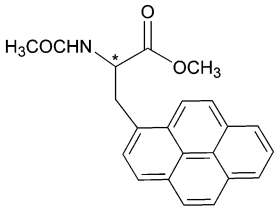

N-acetyl-1-pyrenylalanine methyl ester

60

together with a transient fluorescence spectroscopic study indicated that there was no ground state interaction between these molecules. However, great concentration dependence was observed in the fluorescence spectra of **60**. As the concentration increased from 0.8 mM to 9.6 mM, there was a large increase for the broad excimer emission band at 485 nm. The normal emission maxima were at 377 and 398 nm. The excimer emission maximum was independent of solvent polarity. The dynamics for the excimer emission of the racemic **60** and its enantiomers were investigated. Although no significant rate difference in the formation of the excimers was found, the dissociation from the excimer to the locally excited state between the homotactic L−L and the heterotactic D−L excimers exhibited different rates. The D−L excimer was more stable in inert solvents such as acetonitrile and toluene by 3 kcal/mol ($\Delta H°$) than the L−L excimer. This was attributed to a much better hydrogen-bonding interaction in the heterotactic dimer than in the homotactic dimer.

The excimer formation of **60** in two chiral solvents, (+)-2-octanol (**133**) and (+)-2-chloropropionate methyl ester, was investigated.[77] The excimer emission maximum of both D- and L-**60** in (+)-2-octanol was 484 nm. The excimer formation of L-**60** was ca. 15% more efficient than that of D-**60** in both solvents. Chiral discrimination energies of 0.3 kcal/mol in (+)-2-octanol and 0.2 kcal/mol in (+)-2-chloropropionate were determined. This was attributed to the different tendencies of the diastereomeric solute−solvent pairs to form intermolecular excimers.

7.1.2. Intramolecular Excimer and Exciplex Formation

De Schryver and co-workers synthesized *threo*- and *erythro*-*N*-acetyl-1-pyrenylalanyl-1-methyltryptophan methyl ester (**142** and **143**).[78] In these compounds, the pyrene ring and the indole ring were much closer than in **139**. The absorption spectra of **142** and **143** were the same and were analyzed as the superposition of the spectra of *N*-acetyl-1-pyrenylalanine methyl ester (**60**) and 1-methyl-L-tryptophan methyl ester (**144**). The excitation spectra of **142** and **143** were also the same as that of **60** and they were independent of the analysis wavelength at either 470 or 500 nm. When the solution of **142** or **143** was excited at 343 nm, the ^1L_a transition of the pyrene, in addition to the locally excited state emission at 377 and 396 nm, a broad new band appeared at longer wavelengths in polar solvents such as ethyl acetate and acetonitrile. This new band was attributed to the emission of an intramolecular exciplex formed by the pyrene−indole interaction as the concentration of **142** or **143** was below 10^{-5} M. Compound **143** showed much more intense exciplex emission than **142**. For example, in ethyl acetate, the quantum yield of the exciplex (Φ_{exc}) versus that of the locally excited pyrenyl (Φ_{py}) was 0.44 for **143** and 0.14 for **142**. In acetonitrile, Φ_{exc}/Φ_{py} was 1.55 for **143** and 0.75 for **142**. Little exciplex emission was observed in the less polar solvents such as toluene and diethyl ether. The dipole moment of the exciplex was calculated to be $\mu = 10$ D. The differences observed in the exciplex of the two diastereomeric compounds were attributed to a larger steric hindrance for **142** to achieve a folded conformation than **143**.

The diastereomeric *threo*- and *erythro*-*N*-acetyl-bis-(1-pyrenylalanine) methyl ester (**145a**,**b**) were studied.[79,80] The UV spectra of the two diastereomers were the same and very similar to that of *N*-acetyl-1-pyrenylalanine ethyl ester (**60**) recorded in diethyl ether. The excitation spectra of **145a**,**b** observed at 500 nm showed only methyl pyrene absorption. These indicated no ground state interaction between the two pyrenyl rings in these compounds. They found that these two diastereomeric compounds gave different intramolecular excimer emissions with the maxima at 465 nm for **145b** and 455 nm for **145a** besides the locally excited emission of the pyrenyl at 377 and 396 nm as observed in **60**. In various solvents, **145b** exhibited much more intense excimer emission than **145a**. In DMF, the quantum yield of the excimer (Φ_{exc}) versus that of the locally excited pyrenyl (Φ_{py}) was 0.50 for **145b** (total quantum yield 0.49) and 0.17 for **145a** (total quantum yield 0.28). In methylene chloride, Φ_{exc}/Φ_{py} was 3.0 for **145b**

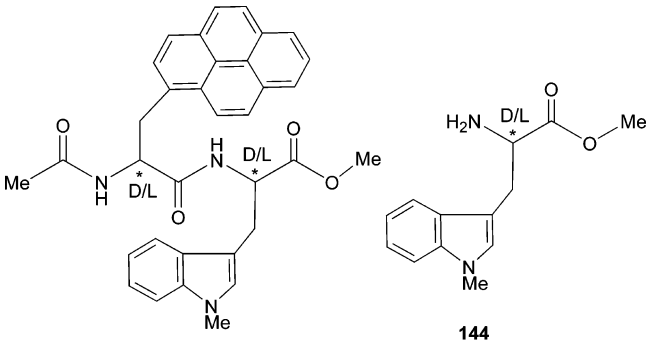

144

DD and LL: threo, **142**
DL and LD: erythro, **143**

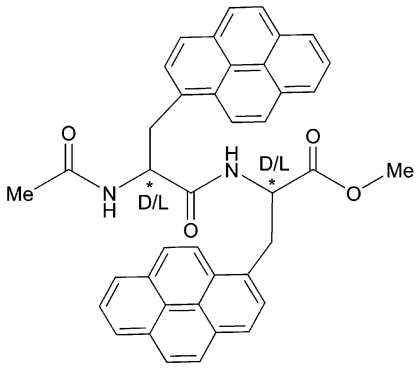

dipeptide N-acetylbis(1 -pyrenylalanine) methyl ester

DD and LL: threo, **145a**
DL and LD: erythro, **145b**

(total quantum yield 0.35) and 1.0 for **145a** (total quantum yield 0.32). The higher component of the excimer emission of **145b** suggested that the conformation of this diastereomer should make it much easier to achieve the excimer geometry within the lifetime of the excited pyrenyl. In DMF, the intermolecular hydrogen bonds between the dipeptide and the hydrogen bond acceptor solvent reduced the intramolecular excimer formation, whereas in methylene chloride, the intramolecular hydrogen bonds supported the excimer formation. However, in alcohols such as the hydrogen bond donor solvent trifluoroethanol, Φ_{exc}/Φ_{py} increased to 8.4 for **145b** and 2.9 for **145a**. The dynamics of the conformation equilibriums of these compounds were studied by the transient fluorescence measurement.

The *meso*- and racemic bis[1-(1-pyrenyl)ethyl] ether (**146**) were synthesized and isolated.[81] The absorption spectrum of **146** in isooctane was very similar to those of pyrene and another analogue 1-(1-pyrenyl)-ethyl ethyl ether (**147**). However, major differences

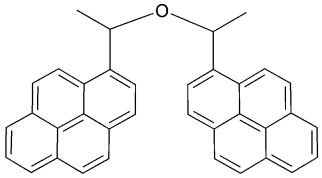

146

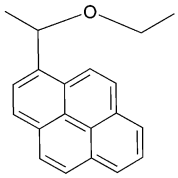

147

were observed in the fluorescence spectra. Unlike the structured monomer emission of **147**, *meso*-**146** (10^{-6} M in isooctane) gave a broad and structureless excimer emission at 472 nm with a complete absence of the monomer emission. The racemic mixture of **147** (10^{-6} M in isooctane) gave both the monomer emission and a weaker excimer emission ($\lambda_{emi} = 512$ nm). Two excimer configurations of *meso*-**146** were observed by the time-correlated single photon counting experiment with two decay times of 93 and 59 ns.

Kano et al. reported the chiral pyrene excimer formation in the cavity of γ-cyclodextrin.[82] Pyrene in dilute aqueous solution showed only monomer emission. Addition of γ-cyclodextrin (1×10^{-2} M) to pyrene (2×10^{-6} M) produced a broad excimer fluorescence band at 474 nm at the expense of the monomer emission. This excimer emission maximum of pyrene in γ-cyclodextrin was of longer wavelength than those found in organic solutions (462−467 nm). A highly intense CPL signal (g_{lum} up to 0.012) was observed for the excimer. Almost no CPL signal was found in the monomer emission region. Previously, pyrene was demonstrated to form 2:1 and/or 2:2 complexes with γ-cyclodextrin, but only weak induced circular dichroism of the pyrene dimer in γ-cyclodextrin was observed ($g_{abs} = \Delta\epsilon/\epsilon = 6 \times 10^{-5}$).[83] That is, the ground state dimer of pyrene inside γ-cyclodextrin had a weak asymmetric nature. Upon excitation, a reoriented and asymmetrically twisted pyrene dimer in γ-cyclodextrin might have been generated giving the large CPL signal.

Interaction of 1,3-bis(1-pyrenyl)propane (**148**) with γ-cyclodextrin was examined. Compound **148** was completely insoluble in water, and its dilute aqueous dispersion (10^{-6} M) gave only excimer like emission at 478 nm, which was attributed to **148** aggregates.

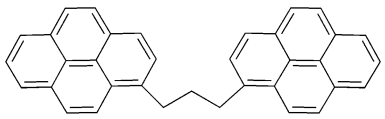

148

In the presence of γ-cyclodextrin (10^{-2} M), emissions due to the locally excited state of **148** as well as its intramolecular excimer ($\lambda_{emi} = 490$ nm) were observed. The g_{lum} of the excimer was 0.003 significantly smaller than that of pyrene-γ-cyclodextrin complex. Evidence for the formation of an intramolecular dimer ground state of **148** inside the γ-cyclodextrin cavity was obtained. This dimer could not reorient upon excitation because of the propylene linkage which might account for its much smaller g_{lum}.

Sisido and co-workers synthesized the optically active block copolymers **149a**,**b** and the optically inactive block copolymer **150**.[84] In these materials, the optically inactive (γ-benzyl DL-glutamate) blocks were introduced to make the resulting polymers soluble. The CD spectra of **149a**,**b** in DMF displayed

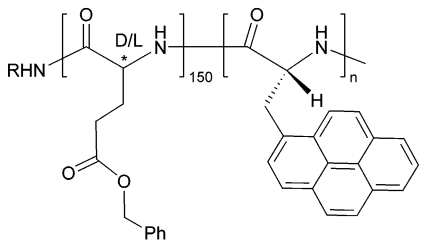

149a: n = 8
149b: n = 20

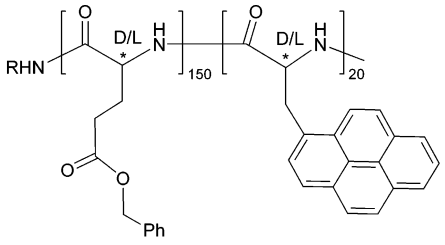

150

1 order of magnitude more intense signals than L-**60**, indicating a helical arrangement of the pyrene units in the chiral polymers. The signals of **149b** were slightly more intense than those of **149a**. The UV absorption and CD signals of the polymers were red-shifted to those of L-**60**. This was attributed to an interchromophoric interaction along the helical polymer chain. In DMF solution at a concentration of 10^{-5} M (based on the pyrene unit), polymers **149a**,**b** and **150** showed both monomer and intramolecular excimer emissions, but L-**60** only gave the monomer emission. The quantum yields of the monomer emission versus the excimer emissions were 0.053/0.198 for **150**, 0.108/0.126 for **149a**, and 0.047/0.073 for **149b**. The optically inactive **150** had the highest excimer as well as overall emissions among the

polymers. The quantum yield of the monomer L-**60** was 0.487, much larger than those of the polymers. The higher molecular weight polymer **149b** had a lower quantum yield than **149a**. The fluorescence detected circular dichroism, circular polarized fluorescence, and time-resolved fluorescence of the optically active polymers and monomers were studied, and revealed detailed information about the emission states of these materials.

7.2. Naphthyl Derivatives

De Schryver et al. prepared *meso*- and racemic bis-[1-(1-naphthyl)ethyl] ether (**151**) and found these compounds to have very different fluorescence spectra.[85] Racemic **151** (10^{-4} M in isooctane) gave both

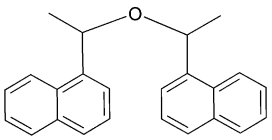

151

the localized monomer and intramolecular excimer (λ_{emi} = 385 nm) emissions with quantum yields of 0.030 and 0.065, respectively. The quantum yields for the monomer and excimer (λ_{emi} = 405 nm) emissions of *meso*-**151** (10^{-4} M in isooctane) were approximately 0.003 and 0.014, respectively. The ratio of the intramolecular excimer emission of *meso*-**151** versus its monomer emission was much higher than that of racemic **151**.

The tetrablock copolymer **152** was prepared by Sisido et al. in which the achiral portions were introduced to make the polynaphthylalanine soluble in organic solvents.[86] The helical arrangement of the

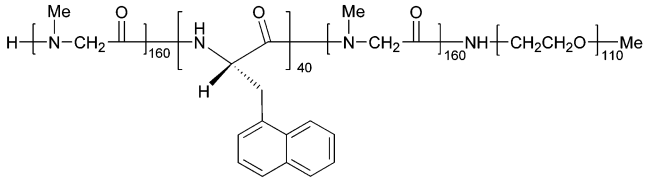

152

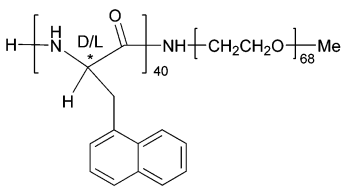

153

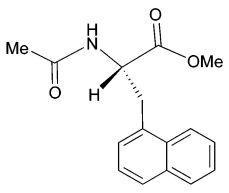

154

naphthyl groups in the polymer gave rise to strong electronic interactions. The UV spectrum of the polymer in trimethyl phosphate solution showed red shifts over that of the monomer **154**. The polymer also had much more intense CD signals. The fluorescence spectra of **152**, **153**, and **154** (10^{-5} M in trimethyl phosphate) displayed a predominantly monomer emission with very small excimer emissions from the polymers. The excimer emission from the optically inactive **153** was a little larger than the optically active **152**. The very small excimer emissions of the naphthyl polymers compared with the intense excimer emissions from the pyrenyl polymers [**149a**,**b** and **150**] indicated a bigger chromophore distance (>4 Å) in the naphthyl polymers.

8. Miscellaneous Studies

8.1. Using Fluorescence Anisotropy in Chiral Recognition

Emission from a fluorescent molecule is polarized when excited with polarized light. Measurement of this fluorescence anisotropy could reveal the size sensitive rotational motion of the fluorescent molecule. A larger sized fluorophore would lead to a slower rotational correlation time and thus a higher anisotropy value. Complexation of a chiral host with a chiral guest molecule would lead to two diastereomeric complexes of different stability and size that could be distinguished by fluorescence anisotropy. Warner and co-workers studied the fluorescence anisotropy of the two enantiomers of several chiral fluorophores including BINOL (**30**), 1,1′-bi-2-naphthyl-2,2′-diamine (BINAM, **33**), 1,1′-bi-2-naphthyl-2,2′-diyl hydrogen phosphate (BINP, **73**), and Troger's base in the presence of (L,L)poly(sodium undecanoyl leucyl-leucinate) (L-PL).[87] They used the term β in the following equation to represent the enantioselective fluorescent anisotropy:

$$r_S/r_R = [3\cos^2\beta - 1]/2$$

where r_S and r_R are the anisotropy values of the *S* and *R* fluorophores in the presence of the chiral guest. The β values for the compounds BINOL, BINAM, BINP, and Troger's base were found to be 4.5, 7.1, 17.8, and 24.2, respectively, in the presence of L-PL. Using the β value, the authors were able to determine the free energy difference of the diastereomeric host−guest complexes according to the following expression:

$$\Delta(\Delta G)_{S,R} = -RT\ln(m\beta + 1)$$

8.2. Kinetic Resolution of Chiral Fluorophores in ee Determination

Shair and co-workers used the pseudoenantiomeric fluorophores **155** and **156** to determine the ee (enantiomeric excess) of amino acids bounded on glass slides in microarrays.[88] Since the two enantiomers of the amino acids reacted with **155** and **156** to form amides with different rates, this kinetic resolution allowed the use of the fluorescence of **155** and **156** to determine the enantiomeric composition. Excitation of **155** at 532 nm gave green emission, and excitation of **156** at 635 nm gave red emission. Mixing the emissions of **155** and **156** at the same intensity gave a yellow color. The following equation was used to calculate the ee from the fluorescence measurement:

$$\%\ \text{ee} = \left[\frac{(\chi - 1)(s + 1)}{(\chi + 1)(s - 1)}\right] \times 100\%$$

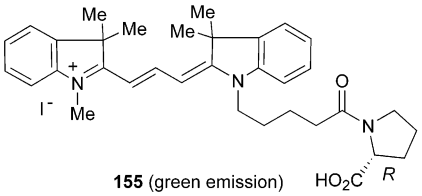

155 (green emission)

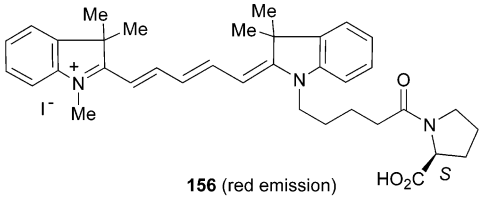

156 (red emission)

where

$$\chi = \frac{I_{\mathbf{156}}}{I_{\mathbf{155}}}\frac{1}{z}$$

and

$$s = \frac{k_{\text{fast}}}{k_{\text{slow}}}$$

In the equation, $I_{\mathbf{155}}$ and $I_{\mathbf{156}}$ are the fluorescence intensity of **155** and **156** when bounded to the amino acids; z is the fluorescence intensity ratio of equimolar **155** and **156** and represents the racemate fluorescence intensity ratio; s is the kinetic resolution factor and can be obtained from the fluorescence measurement of samples with known ee.

Using this method, the authors were able to quickly identify the samples with high ee's out of 15552 amino acids bound to glass slides.

8.3. Imprinting of Chiral Fluorophores in Sol–Gel Films

Marx and co-workers used an indirect fluorescent assay to study the sol−gel thin films imprinted with chiral molecules such as **157** and **158**.[89] The enantiomerically pure molecules were combined with

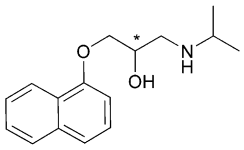

(*R*)-**157**
(*S*)-**157**

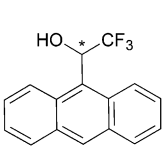

(*R*)-**158**
(*S*)-**158**

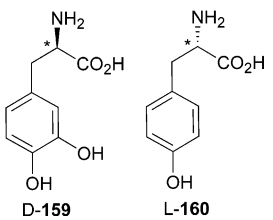

D-**159**

L-**160**

various alkoxysilanes including tetramethoxysilane, tetraethoxysilane, phenyl trimethoxysilane, and 3-aminopropyltriethoxysilane which upon hydrolysis and extraction of the chiral templates generated the chirally imprinted films. These imprinted films were then used to interact with the enantiomers of **157** and **158**. The enantioselective adsorptions were then analyzed by extracting the adsorbed molecules from the films and measuring their fluorescence intensity. The D- and L-**159** imprinted films were also used to interact with the radio-labeled L-**160**, and the radioactivity was used to analyze the adsorption. These studies showed a certain degree of enantioselective adsorption by the imprinted sol−gel films.

9. Summary

The studies of organic molecules in enantioselective fluorescent recognition are summarized in this article. The most investigated chiral fluorophores are those containing 1,1′-binaphthyl units. Because of their unique chiral configuration and fluorescence properties, 1,1′-binaphthyl compounds have been used in the recognition of a great variety of chiral molecules including amines, amino alcohols, amino acids, α-hydroxycarboxylic acids, and sugars. Highly enantioselective responses in both fluorescence quenching and enhancement have been observed in a few cases. Another promising class of chiral fluorescent receptors is derived from cyclodextrins containing fluorescent tags. Binding of a chiral guest molecule inside the chiral cavity of these cyclodextrin derivatives can generate enantioselective responses from their fluorophores. Other chiral receptors including helicenes, calixarenes, crown ethers, proteins, and enzymes have also exhibited various degrees of chiral recognition in fluorescence. Chiral amines, amino alcohols, amino acids, α-hydroxycarboxylic acids, and monosaccharides are the main guest molecules investigated in this area. A majority of these compounds contain either a nitrogen atom that can quench the emission of a fluorophore or an acid group that can enhance the fluorescence by protonation of the nitrogen atoms of the fluorophore. Fluorescent recognition of other chiral molecules such as simple alcohols, ketones, and alkenes still remains a very challenging task despite the promising work of using cyclodextrin-based fluorophores.

One driving force behind the recent activity in the study of enantioselective fluorescent sensors is to develop a real time analytical tool for chiral assay. This method in combination with combinatorial chiral catalyst screening and asymmetric synthesis should be of great value to general organic synthesis as well as pharmaceutical synthesis. One of the current challenges for the practical use of enantioselective fluorescent sensors is to be able to determine the enantiomeric composition of chiral molecules on either heterogeneous or homogeneous supports. Recognition of the supported substrates could allow the fluorescence measurements to be conducted in the absence of catalysts, reagents or other impurities after the chiral molecules are generated from the combinatorial synthesis.

10. Acknowledgment

We are grateful for the support provided by the National Institutes of Health (R01GM58454/R01EB002037-05) for our work in this area.

11. References

(1) *Fluorescent Chemosensors for Ion and Molecular Recognition*; Czarnik, A. W., Ed.; ACS Symposium Series 538; American Chemical Society: Washington, DC, 1993.
(2) de Silva, A. P.; Gunaratne, H. Q. N.; Gunnlaugsson, T.; Huxley, A. J. M.; McCoy, C. P.; Rademacher, J. T.; Rice, T. E. *Chem. Rev.* **1997**, *97*, 1515.
(3) Fabbrizzi, L.; Poggi, A. *Chem. Soc. Rev.* **1995**, *24*, 197.
(4) *Fluorescent and Luminescent Probes*, 2nd ed.; Mason, W. T., Ed.; Academic: San Diego, 1999.
(5) Reviews: (a) Finn, M. G. *Chirality* **2002**, *14*, 534. (b) Reetz, M. T. *Angew. Chem., Int. Ed.* **2002**, *41*, 1335. (c) Tsukamoto, M.; Kagan, H. B. *Adv. Synth. Catal.* **2002**, *344*, 453.
(6) (a) Guo, J.; Wu, J.; Siuzdak, G.; Finn, M. G. *Angew. Chem., Int. Ed.* **1999**, *38*, 1755. (b) Reetz, M. T.; Becker, M. H.; Klein. H.-W.; Stöckigt, D. *Angew. Chem., Int. Ed.* **1999**, *38*, 1758. (c) Reetz, M. T.; Becker, M. H.; Kuhling, K. M.; Holzwarth, A. *Angew. Chem., Int. Ed.* **1998**, *37*, 2647.
(7) Reetz, M. T.; Kuhling, K. M.; Deege, A.; Hinrichs, H.; Belder, D. *Angew. Chem., Int. Ed.* **2000**, *39*, 3891.
(8) Abato, P.; Seto, C. T. *J. Am. Chem. Soc.* **2001**, *123*, 9206.
(9) Ding, K.; Ishii, A.; Mikami, K. *Angew. Chem., Int. Ed.* **1999**, *38*, 497.
(10) Rau, H.; Ratz, R. *Angew. Chem., Int. Ed. Engl.* **1983**, *22*, 550.
(11) (a) Metcalf, D. H.; Snyder, S. W.; Demas, J. N.; Richardson, F. S. *J. Am. Chem. Soc.* **1990**, *112*, 5681. (b) Metcalf, D. H.; Stewart, J. M. M.; Snyder, S. W.; Grisham, C. M.; Richardson, F. S. *Inorg. Chem.* **1992**, *31*, 2445. (c) Glover-Fischer, D. P.; Metcalf, D. H.; Hopkins, T. A.; Pugh, V. J.; Chisdes, S. J.; Kankare, J.; Richardson, F. S. *Inorg. Chem.* **1998**, *37*, 3026.
(12) Bolender, J. P.; Meyers, A.; Cordaro, J.; Ries, R. S. *Chirality* **2002**, *14*, 456.
(13) Rexwinkel, R. B.; Meskers, S. C. J.; Dekkers, H. P. J. M.; Riehl, J. P. *J. Phys. Chem.* **1992**, *96*, 5725.
(14) Corradini, R.; Sartor, G.; Marchelli, R.; Dossena, A.; Spisni, A. *J. Chem. Soc., Perkin Trans. 2* **1992**, 1979.
(15) Glover-Fischer, D. P.; Metcalf, D. H.; Bolender, J. P.; Richardson, F. S. *Chem. Phys.* **1995**, *198*, 207.
(16) Meskers, S. C. J.; Dekkers, H. P. J. M. *J. Am. Chem. Soc.* **1998**, *120*, 6413.
(17) Meskers, S. C. J.; Dekkers, H. P. J. M. *J. Phys. Chem. A.* **2001**, *105*, 4589.
(18) Meskers, S. C. J.; Dekkers, H. P. J. M.; Rapenne, G.; Sauvage, J. P. *Chem. Eur. J.* **2000**, *6*, 2129.
(19) (a) Parker, D.; Dickins, R. S.; Puschmann, H.; Crossland, C.; Howard, J. A. K. *Chem. Rev.* **2002**, *102*, 1977. (b) Tsukube, H.; Shinoda, S.; Tamiaki, H. *Coord. Chem. Rev.* **2002**, *226*, 227.
(20) (a) Aspinall, H. C. *Chem. Rev.* **2002**, *102*, 1807. (b) Tsukube, H.; Shinoda, S. *Chem. Rev.* **2002**, *102*, 2389.
(21) Irie, M.; Yorozu, T.; Hayashi, K. *J. Am. Chem. Soc.* **1978**, *100*, 2236.
(22) Lakowicz, J. R. *Principles of Fluorescence Spectroscopy*, 2nd ed.; Kluwer Academic/Plenum: New York, 1999.
(23) Yorozu, T.; Hayashi, K.; Irie, M. *J. Am. Chem. Soc.* **1981**, *103*, 5480.
(24) Avnir, D.; Wellner, E.; Ottolenghi, M. *J. Am. Chem. Soc.* **1989**, *111*, 2001.
(25) Iwanek, W.; Mattay, J. *J. Photochem. Photobiol., A* **1992**, *67*, 209.
(26) Parker, K. S.; Townshend, A.; Bale, S. J. *Anal. Proc. incl. Anal. Commun.* **1995**, *32*, 329.
(27) Parker, K. S.; Townshend, A.; Bale, S. J. *Anal. Commun.* **1996**, *33*, 265.
(28) Beer, G.; Rurack, K.; Daub, J. *J. Chem. Soc., Chem. Commun.* **2001**, 1138.
(29) Hu, Q.-S.; Pugh, V.; Sabat, M.; Pu, L. *J. Org. Chem.* **1999**, *64*, 7528.
(30) (a) Pugh, V.; Hu, Q.-S.; Pu, L. *Angew. Chem., Int. Ed.* **2000**, *39*, 3638. (b) Pugh, V.; Hu, Q.-S.; Zuo, X.-B.; Lewis, F. D.; Pu, L. *J. Org. Chem.* **2001**, *66*, 6136.
(31) Gong, L.-Z.; Hu, Q.-S.; Pu, L. *J. Org. Chem.* **2001**, *66*, 2358.
(32) Wang, D.; Liu, T.-J.; Zhang, W.-C.; Slaven, W. T., IV; Li, C.-J. *J. Chem. Soc., Chem. Commun.* **1998**, 1747.
(33) Liu, T. J.; Chen, Y. J.; Zhang, K. S.; Wang, D.; Guo, D. W.; Yang, X. Z. *Chirality* **2001**, *13*, 595.
(34) Ma, L.; White, P. S.; Lin, W.-B. *J. Org. Chem.* **2002**, *67*, 7577.
(35) Zhang, H.-C.; Pu, L. Manuscript submitted.
(36) Lee, S. J.; Lin, W.-B. *J. Am. Chem. Soc.* **2002**, *124*, 4554.
(37) Raut, H.; Tottertf, F. *J. Photochem. Photobiol., A* **1992**, *63*, 337.
(38) Reetz, M. T.; Sostmann, S. *Tetrahedron* **2001**, *57*, 2515.
(39) Grady, T.; Harris, S. J.; Smyth, M. R.; Diamond, D.; Hailey, P. *Anal. Chem.* **1996**, *68*, 3775.
(40) Grady, T.; Joyce, T.; Smyth, M. R.; Harris, S. J.; Diamond, D. *Anal. Commun.* **1998**, *35*, 123.
(41) Fox, M. A.; Singletary, N. J. *Tetrahedron Lett.* **1979**, *20*, 2189.
(42) López-Arbeloa, F.; van der Auweraer, M.; Ruttens, F.; De Schryver, F. C. *J. Photochem. Photobiol., A* **1988**, *44*, 63.
(43) Prodi, L.; Bolletta, F.; Montalti, M.; Zaccheroni, N.; Huszthy, P.; Samu, E.; Vermes, B. *New J. Chem.* **2000**, *24*, 781.
(44) (a) Brunner, H.; Schiessling, H. *Angew Chem., Int. Ed. Engl.* **1994**, *33*, 125. (b) Brunner, H.; Schiessling, H. *Bull. Soc. Chim. Belg.* **1994**, *103*, 119.
(45) Lin, J.; Zhang, H.-C.; Pu, L. *Org. Lett.* **2002**, *4*, 3297.
(46) (a) Lin, J.; Li, Z.-B.; Zhang, H.-C.; Pu, L. *Tetrahedron Lett.* **2004**, *45*, 103. (b) Li, Z.-B.; Lin, J.; Zhang, H.-C.; Pu, L. Manuscript submitted.
(47) Murakoshi, K.; Azechi, T.; Hosokawa, H.; Wada, Y.; Yanagida, S. *J. Electroanal. Chem.* **1999**, *473*, 117−124.
(48) Tundo, P.; Fendler, J. H. *J. Am. Chem. Soc.* **1980**, *102*, 1760−1762. The captions of Figure 2 and Figure 3 in this paper should be interchanged.
(49) Ueno, A.; Suzuki, I.; Osa, T. *J. Am. Chem. Soc.* **1989**, *111*, 6391.
(50) Ueno, A.; Suzuki, I.; Osa, T. *Anal. Chem.* **1990**, *62*, 2461.
(51) Ueno, A.; Kuwabara, T.; Nakamura, A.; Toda, F. *Nature* **1992**, *356*, 136.
(52) Pagliari, S.; Corradini, R.; Galaverna, G.; Sforza, S.; Dossena, A.; Marchelli, R. *Tetrahedron Lett.* **2000**, *41*, 3691.
(53) Yang, H.; Bohne, C. *J. Photochem. Photobiol., A* **1995**, *86*, 209.
(54) Godoy-Alcántar, C.; Nelen, M. I.; Eliseev, A. V.; Yatsimirsky, A. K. *J. Chem. Soc., Perkin Trans. 2* **1999**, 353.
(55) Yan, Y.; Myrick, M. L. *Anal. Chem.* **1999**, *71*, 1958.
(56) Abe, Y.; Fukui, S.; Koshiji, Y.; Kobayashi, M.; Shoji, T.; Sugata, S.; Nishizawa, H.; Suzuki, H.; Iwata, K. *Biochim. Biophys. Acta* **1999**, *1433*, 188.
(57) Abe, Y.; Shoji, T.; Matsubara, M.; Yoshida, M.; Sugata, S.; Iwata, K.; Suzuki, H. *Chirality* **2000**, *12*, 565.
(58) Kumar, C. V.; Buranaprapuk, A.; Sze, H. C. *Chem. Commun.* **2001**, 297.
(59) (a) Gafni, A. *J. Am. Chem. Soc.* **1980**, *102*, 7367. (b) Gafni, A. *Biochemistry* **1979**, *18*, 1540.
(60) Corradini, R.; Sartor, G.; Marchelli, R.; Dossena, A.; Spisni, A. *J. Chem. Soc., Perkin Trans. 2* **1992**, 1979.
(61) Lin, J.; Hu, Q.-S.; Xu, M. H.; Pu, L. *J. Am. Chem. Soc.* **2002**, *124*, 2088.
(62) Xu, M.-H.; Lin, J.; Hu, Q.-S.; Pu, L. *J. Am. Chem. Soc.* **2002**, *124*, 14239.
(63) (a) Yoon, J.; Czarnik, A. W. *J. Am. Chem. Soc.* **1992**, *114*, 5874. (b) James, T. D.; Sandanayake, K. R. A. S.; Shinkai, S. *Angew. Chem., Int. Ed. Engl.* **1996**, *35*, 1910.
(64) James, T. D.; Sandanayake, K. R. A. S.; Shinkai, S. *Nature* **1995**, *374*, 345−347. de Silva, A. P. *Nature* **1995**, *374*, 310.
(65) Takeuchi, M.; Yoda, S.; Imada, T.; Shinkai, S. *Tetrahedron* **1997**, *53*, 8335.
(66) Hamasaki, K.; Ikeda, H.; Nakamura, A.; Ueno, A.; Toda, F.; Suzuki, I.; Osa, T. *J. Am. Chem. Soc.* **1993**, *115*, 5035.
(67) Ueno, A.; Suzuki, I.; Osa, T. *Anal. Chem.* **1990**, *62*, 2461.
(68) Ueno, A.; Minato, S.; Osa, T. *Anal. Chem.* **1992**, *64*, 1154.
(69) Corradini, R.; Dossena, A.; Marchelli, R.; Panagia, A.; Sartor, G.; Saviano, M.; Lombardi, A.; Pavone, V. *Chem. Eur. J.* **1996**, *2*, 373.
(70) Al-Rabaa, A. R.; Bréhéret, E.; Lahmani, F.; Zehnacker, A. *Chem. Phys. Lett.* **1995**, *237*, 480.
(71) Al-Rabaa, A. R.; Le Barbu, K.; Lahmani, F.; Zehnacker-Rentien, A. *J. Phys. Chem. A* **1997**, *101*, 3273.
(72) Lahmani, F.; Le Barbu, K.; Zehnacker-Rentien, A. *J. Phys. Chem. A* **1999**, *103*, 1991.
(73) Sampath, D. S.; Balaram, P. *Biochim. Biophys. Acta* **1986**, *882*, 183.
(74) Tran, C. D.; Fendler, J. H. *J. Am. Chem. Soc.* **1980**, *102*, 2923.
(75) Brittain, H.; Ambrozich, D. L.; Saburi, M.; Fendler, J. H. *J. Am. Chem. Soc.* **1980**, *102*, 6372.
(76) López-Arbeloa, F.; Goedeweeck, R.; Ruttens, F.; De Schryver, F. C.; Sisidot, M. *J. Am. Chem. Soc.* **1987**, *109*, 3068.
(77) López-Arbeloa, F.; van der Auweraer, M.; Ruttens, F.; de Schryver, F. C. *J. Photochem. Photobiol., A* **1988**, *44*, 133.
(78) Ruttens, F.; Goedeweeck, R.; Lopez-Arbeloa, F.; De Schryver, F. C. *Photochem. Photobiol.* **1985**, *42*, 341.
(79) Goedeweeck, R.; De Schryver, F. C. *Photochem. Photobiol.* **1984**, *39*, 515.
(80) Goedeweeck, R.; Van der Auweraer, M.; De Schryver, F. C. *J. Am. Chem. Soc.* **1985**, *107*, 2334.
(81) Collart, P.; Demeyer, K.; Toppet, S.; De Schryver, F. C. *Macromolecules* **1983**, *16*, 1390.
(82) Kano, K.; Matsumoto, H.; Hashimoto, S.; Sisido, M.; Imanishi, Y. *J. Am. Chem. Soc.* **1985**, *107*, 6117.
(83) Kobayashi, N.; Saito, R.; Hino, H.; Hino, Y.; Ueno, A.; Osa, T. *J. Chem. Soc., Perkin Trans. 2* **1983**, 1031.
(84) Egusa, S.; Sisido, M.; Imanishi, Y. *Macromolecules* **1985**, *18*, 882.
(85) De Schryver, F. C.; Demeyer, K.; Toppet, S. *Macromolecules* **1983**, *16*, 89.
(86) Sisido, M.; Egusa, S.; Imanishi, Y. *J. Am. Chem. Soc.* **1983**, *105*, 1041.

(87) McCarroll, M. E.; Billiot, F. H.; Warner, I. M. *J. Am. Chem. Soc.* **2001**, *123*, 3173.
(88) Korbel, G. A.; Lalic, G.; Shair, M. D. *J. Am. Chem. Soc.* **2001**, *123*, 361.
(89) Fireman-Shoresh, S.; Avnir, D.; Marx, S. *Chem. Mater.* **2003**, *15*, 3607.

CR030052H